



U.S. Department
of Transportation
**National Highway
Traffic Safety
Administration**



DOT HS 812 743

July 2019

Small Female/Older Occupant Thoracic Biofidelity Corridor Development

DISCLAIMER

This publication is distributed by the U.S. Department of Transportation, National Highway Traffic Safety Administration, in the interest of information exchange. The opinions, findings and conclusions expressed in this publication are those of the authors and not necessarily those of the Department of Transportation or the National Highway Traffic Safety Administration. The United States Government assumes no liability for its contents or use thereof. If trade or manufacturers' names are mentioned, it is only because they are considered essential to the object of the publication and should not be construed as an endorsement. The United States Government does not endorse products or manufacturers.

Suggested APA Format Citation:

Crandall, J. R., Shaw, C. G., Forman, J. L., Kerrigan, J. R., Ash, J., & Bollapragada, V. (2019, July). *Small female/older occupant thoracic biofidelity corridor development* (Report No. DOT HS 812 743). Washington, DC: National Highway Traffic Safety Administration.

Technical Report Documentation Page

1. Report No. DOT HS 812 743	2. Government Accession No.	3. Recipient's Catalog No.	
4. Title and Subtitle Small Female/Older Occupant Thoracic Biofidelity Corridor Development	5. Report Date July 2019		6. Performing Organization Code
	8. Performing Organization Report No.		
7. Authors Jeff R. Crandall, project manager; C. Gregory Shaw, Jason L. Forman, Jason R. Kerrigan, Joseph Ash, Varun Bollapragada	10. Work Unit No. (TRAIS)		
9. Performing Organization Name and Address University of Virginia Center for Applied Biomechanics 4040 Lewis and Clark Dr. Charlottesville, VA 22911	11. Contract or Grant No. DTNH2215D00022 Task Order Number: TO0001		
	13. Type of Report and Period Covered Final Report		
12. Sponsoring Agency Name and Address National Highway Traffic Safety Administration 1200 New Jersey Avenue SE Washington, DC 20590	14. Sponsoring Agency Code		
	15. Supplementary Notes Gold Standard Buck Condition 2.1: 2 kN Force Limited Belt, 30 km/h Frontal; Tests UVAS0209-UVAS0213 and UVAS0370-UVAS0374		
16. Abstract <p>This report presents corridors for the biomechanical response of 10 female cadaver subjects, similar in mass and size to a 5th percentile female, in 30 km/h frontal sled tests performed under the gold standard test conditions. The corridors were based on tests conducted at UVA in 2013 (DTNH22-09-H-00247) and 2016 (DTNH2215D00022). The subjects were classified into healthy and unhealthy based on their bone mineral density with the unhealthy being the osteoporotic specimens with a T-score < -2.5 and the healthy being the osteopenic and normal specimens with a T-score > -2.5. The corridors generated from the test data fall under the following categories:</p> <ol style="list-style-type: none"> 1. Chest deflection corridors relative to T8 coordinate system (based on Vicon data) 2. The displacement of anatomical centers of head, T1, T8, L2 and pelvis (based on Vicon data) 3. Transformed head and T1 acceleration and angular rate sensor data. 4. Belt load, and seat, knee bolster and foot plate load cell data time histories. <p>BioRank metric was used to quantify the difference between the unhealthy and healthy corridors generated in this study. Most of the responses, i.e., kinematics, chest deflection and belt forces, showed a BioRank of less than 1 or close to 1 indicating that the difference in responses of the healthy and unhealthy subjects was less than the inherent variation in responses observed among the healthy test subjects. The data from healthy and unhealthy subjects were then combined to create 'unified' corridors for the signals that were not found to be significantly different between the healthy and unhealthy cohorts.</p>			
17. Key Words 5th percentile female, biomechanical response, frontal sled test		18. Distribution Statement Document is available to the public from the National Technical Information Service, www.ntis.gov .	
19. Security Classif. (of this report) Unclassified	20. Security Classif. (of this page) Unclassified	21. No. of Pages 55	22. Price

Form DOT F 1700.7 (8-72)

Reproduction of completed page authorized

Table of Contents

Introduction	1
Methods	1
Arc length normalization	1
Point to point standard deviation	5
Data processing and filtering	6
Response corridors	7
Vicon Corridors	8
Buck Load Cell	18
Angular rate	21
Acceleration	23
Comparison of Healthy and Unhealthy Subjects	25
BioRank	25
Permutation Sampling test	26
Unified response corridors	28
Vicon Corridors	28
Belt Forces	38
Buck Load Cell	39
Angular rate	42
Acceleration	44
References	46
Appendix A: Raw data	A-1
Thoracic Deflection (X)	A-1
Displacement of Anatomical Centers (X).....	A-2
Buck Load Cell	A-3
Belt Forces	A-4

Introduction

This report presents corridors for the biomechanical response of 10 female cadaver subjects, similar in mass and size to a 5th percentile female, in 30 km/h frontal sled tests performed under the gold standard test conditions (S0209-S0213, S0370-S0374). The set up describing the gold standard conditions can be found in Ash, Lessley, Forman, Zhang, Shaw, & Crandall (2012). The corridors were based on tests conducted at the University of Virginia in 2013 (Contract No. DTNH22-09-H-00247) and 2016 (Contract No. DTNH2215D00022). The subjects were classified into healthy and unhealthy based on their bone mineral density (BMD) with the unhealthy being the osteoporotic specimens with a T-score < -2.5 (S0210, S0211, S0213, S0370, S0371) and the healthy being the osteopenic and normal specimens with a T-score > -2.5 (S0209, S0212, S0372, S0373, S0374). The corridors generated from the test data fall under the following categories.

1. Chest deflection corridors relative to T8 coordinate system (based on Vicon data)
2. The displacement of anatomical centers of head, T1, T8, L2 and pelvis (based on Vicon data)
3. Transformed head and T1 acceleration and angular rate sensor data
4. Belt load, and seat, knee bolster and foot plate load cell data time histories

BioRank metric was used to quantify the difference between the unhealthy and healthy corridors generated in this study.

Methods

Arc length normalization and point to point standard deviation approach were the two methods adopted to generate the corridors presented in this report.

Arc length normalization

The arc length normalization method has been proposed by Donlon, Jadooki, Toczyski, Lessley, & Forman (2016) at NHTSA's 44th International Workshop on Human Subjects for Biomechanical Research. It is objective in nature meaning that the method is insensitive to the end user and is easier to implement compared to the approach developed by Lessley, Crandall, Shaw, Kent, & Funk (2004).

The curves were parametrized based on the length of their arc. Consider the example time histories shown in Figure 1, anchor points were defined at the start and the peaks of each curve (Figure 2). The length of arc between the two anchor points was used to normalize the length of arc of each individual time history as shown for curve B (Figure 3). For example, consider Figure 3, if the length of the curve B was 5 units, with peak being observed at 0.65 s, the arc length of the curve between the two anchor points ($t=0$ and $t=0.65$ s) is 2.5 units. The total length of the curve is then normalized by the factor 2.5 (arc length between the two anchor points) so that the normalized arc length at peak is equal to 1. The abscissa (T) and ordinate (F) of individual time histories were then transformed into s space (arc length space) (Figure 4). The peaks of the ordinate align in the s space and a variation in the abscissa with increasing arc

length was noticed which generally represents the difference in frequency content in case of time histories (Figure 5). The mean and standard deviation in the abscissa and ordinate values were calculated in the s space. The average from the abscissa and ordinate in the s domain yield the mean curve (Figure 6). The standard deviation in abscissa and ordinate calculated at each point in the s domain is used to generate one standard deviation ellipses around the mean curve. The corridors were generated by joining the outer boundaries of ellipses (Figure 7). If the magnitude of the standard deviation in the abscissa is greater than zero, then the corridor extends further in time than the mean at the end point.

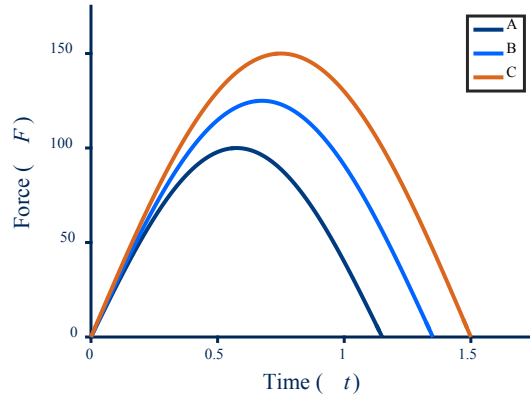


Figure 1. Generic Force time histories

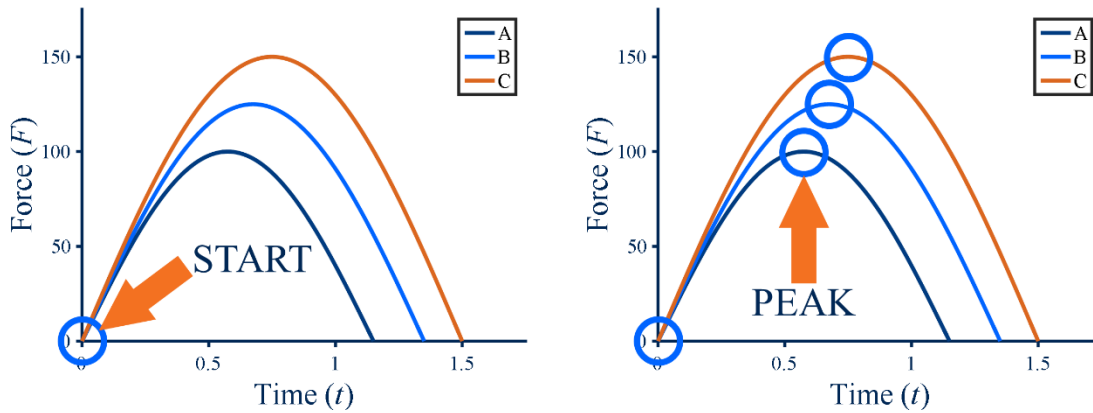


Figure 2. Anchor points

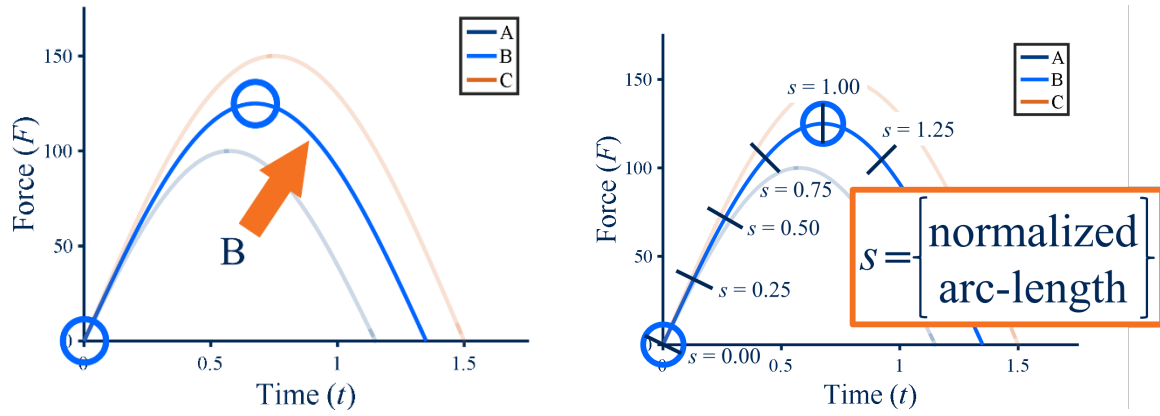


Figure 3. Parametrization

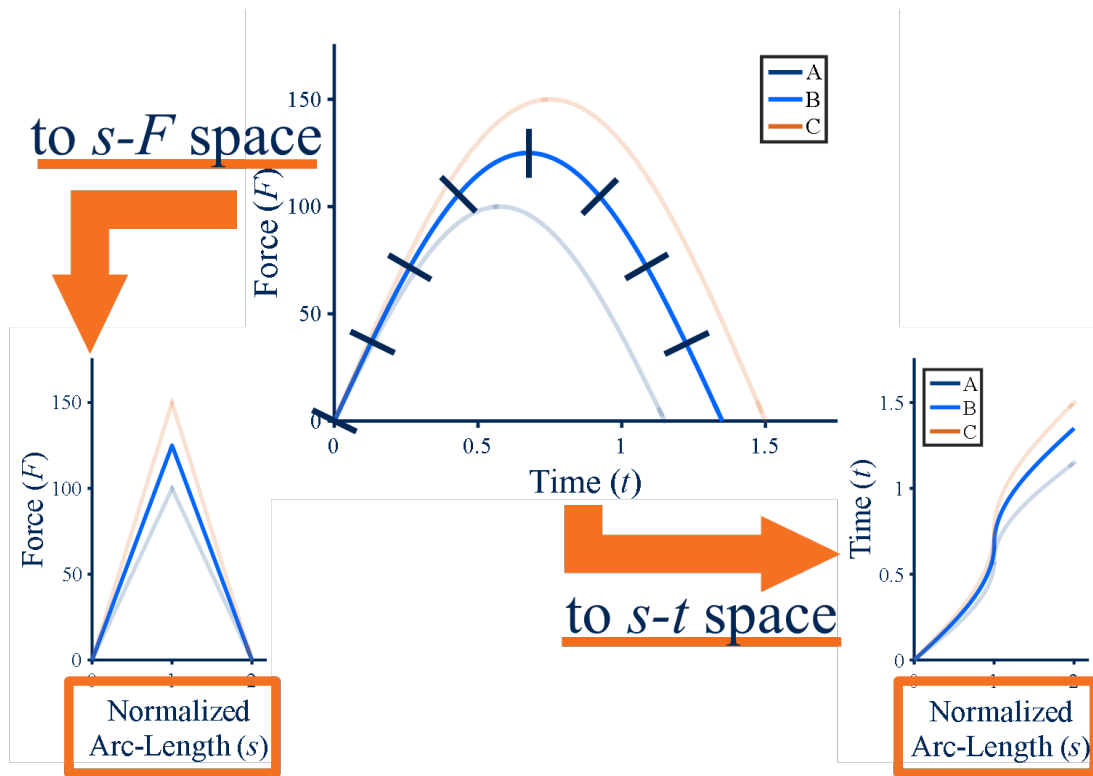


Figure 4. Transformation into s Space.

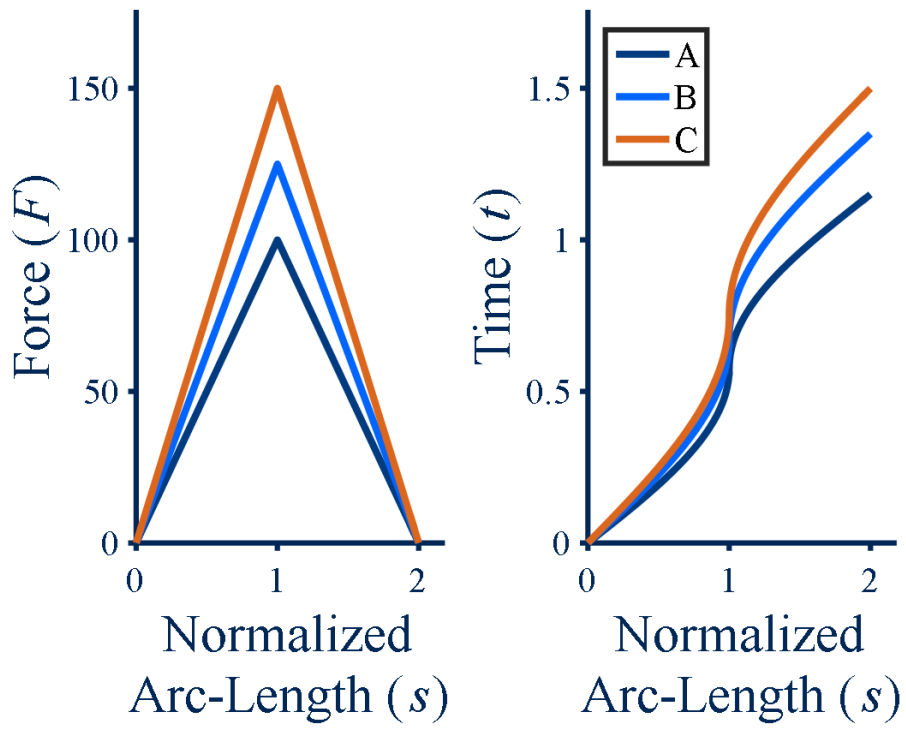


Figure 5. Data in s Space

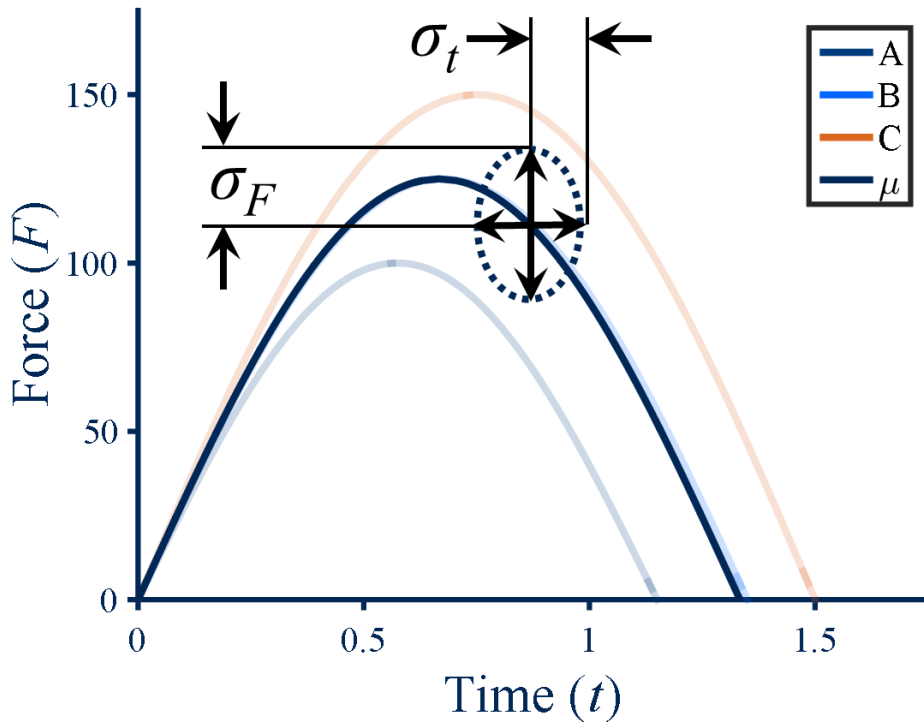


Figure 6. Corridor generation

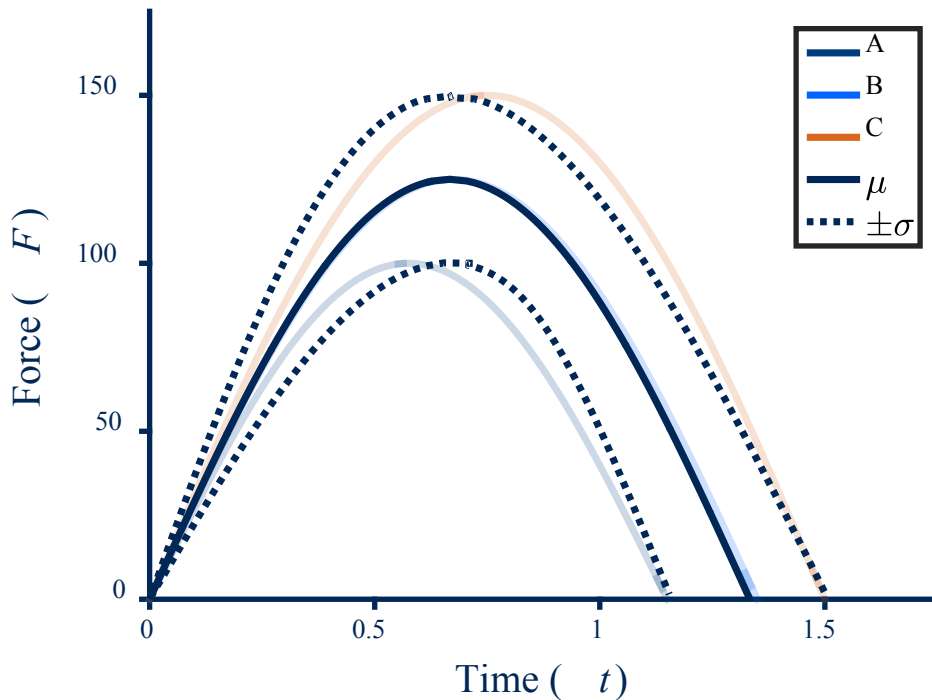


Figure 7. Corridor

The arc length normalization method was employed to generate corridors when the underlying signals had a basic shape that needs to be captured and it was important to quantify the phase and timing of the peaks. Therefore, this method was employed to generate the deflection and displacement corridors in the impact direction (X) as it was the dominant mode. The load cell data and belt load time histories contained a characteristic shape and therefore their corridors were generated using this method and the angular rate of head and T1 anatomical centers.

Point to point standard deviation

The acceleration signals measured at the head and T1 anatomical centers, and the thoracic deflection measures in non-impact directions (Y and Z) were noisy and did not have a basic shape that was necessary to be captured. This problem wasn't observed in cases of displacement of the anatomical centers in non-impact direction as the magnitude of displacement was higher and were less noisy in nature. The arc length method fails generally when there is no underlying shape to the curve as the length of each curve varies proportional to the noise in data which could lead to distortion of data in time domain. Therefore, a more basic methodology described by Rhule, Donnelly, Moorhouse, and Kang (2013) was employed in generating these corridors. The mean curves were obtained by calculating point to point (in time) average of the given time histories. However, it has to be mentioned that cross-correlation and LaGrange multiplier technique was not employed in this study. The time history of standard deviation was obtained at each point in time and was used in generating the upper and lower bounds for the corridor. Rhule and colleagues described the use of an average standard deviation for the entire time history to

avoid a “Necking” problem at the peaks, however, this was deemed unnecessary owing to the chaotic nature of the underlying data.

The methodology used for corridor development of each signal has been summarized in Table 2.

Data processing and filtering

Prior to the creation of corridors, the test data was filtered as shown below.

- Sled load cells – CFC 30, belt gauge CFC 60
- T1 and head accelerometers and angular rate sensors: CFC 60 (to minimize the noise)
- Vicon data: Moving window average (8 point)

Some errors/spikes were recorded in the Vicon data during the data capture phase. These were most likely caused due to the loss of Vicon track ball or the vision to track it for a certain duration of the test. These were estimated by using a linear interpolation of the data between the endpoints (start and end of the error) in Vicon data (Table 1).

Table 1. Spikes or abnormalities in Vicon data

Vicon signal	Subject	Time [ms]
Head Z	S0212	160-180
T1 X	S0370	20-30
T1 Z	S0370	20-30
Pelvis Z	S0370	45-60
Thorax Upper Right X	S0213	150-200
Thorax Upper Right Y	S0213	150-200
Thorax Upper Right Z	S0213	150-200
Thorax Upper Right X	S0374	145-200
Thorax Upper Right Y	S0374	145-200
Thorax Upper Right Z	S0374	145-200
Thorax Lower Right X	S0373	180-200
Thorax Lower Right Y	S0373	180-200
Thorax Lower Right Z	S0373	180-200

Response corridors

*Table 2. Corridor method matrix
(Rhule et al. refers to Rhule, Donnelly, Moorhouse, & Kang (2013))*

Figure	Signal	Corridor Method
8	Sternum deflection X	Arc length
8	Sternum deflection Y/Z	Rhule et al.
9	Thorax Upper Left deflection X	Arc length
9	Thorax Upper Left deflection Y/Z	Rhule et al.
10	Thorax Upper Right deflection X	Arc length
10	Thorax Upper Right deflection Y/Z	Rhule et al.
11	Thorax Lower Left deflection X	Rhule et al.
11	Thorax Lower Left deflection Y/Z	Rhule et al.
12	Thorax Lower Right deflection X	Arc length
12	Thorax Lower Right deflection Y/Z	Rhule et al.
13-17	Displacement of anatomical centers X/Y/Z	Arc length
18-19	Belt Forces	Arc length
20-21	Load cell Forces	Arc length

Vicon Corridors

Thoracic deflection

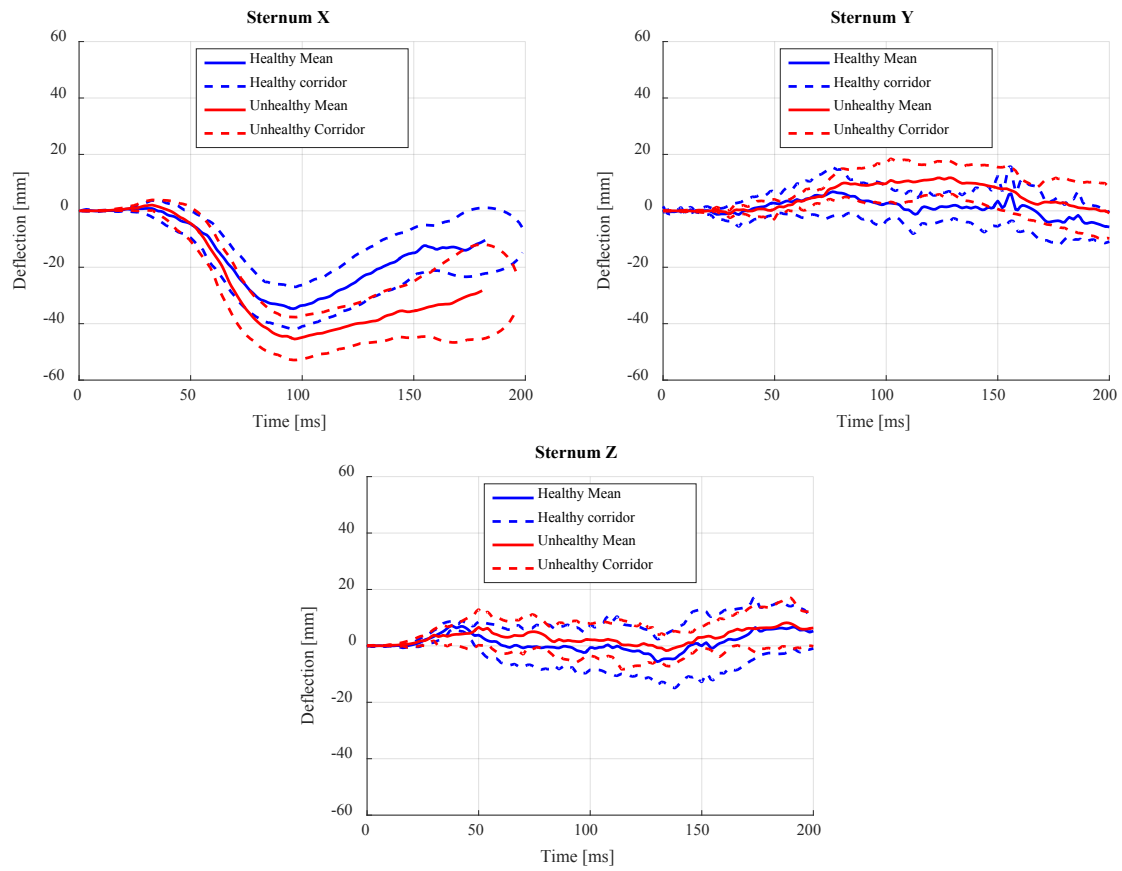


Figure 8. Sternum deflection

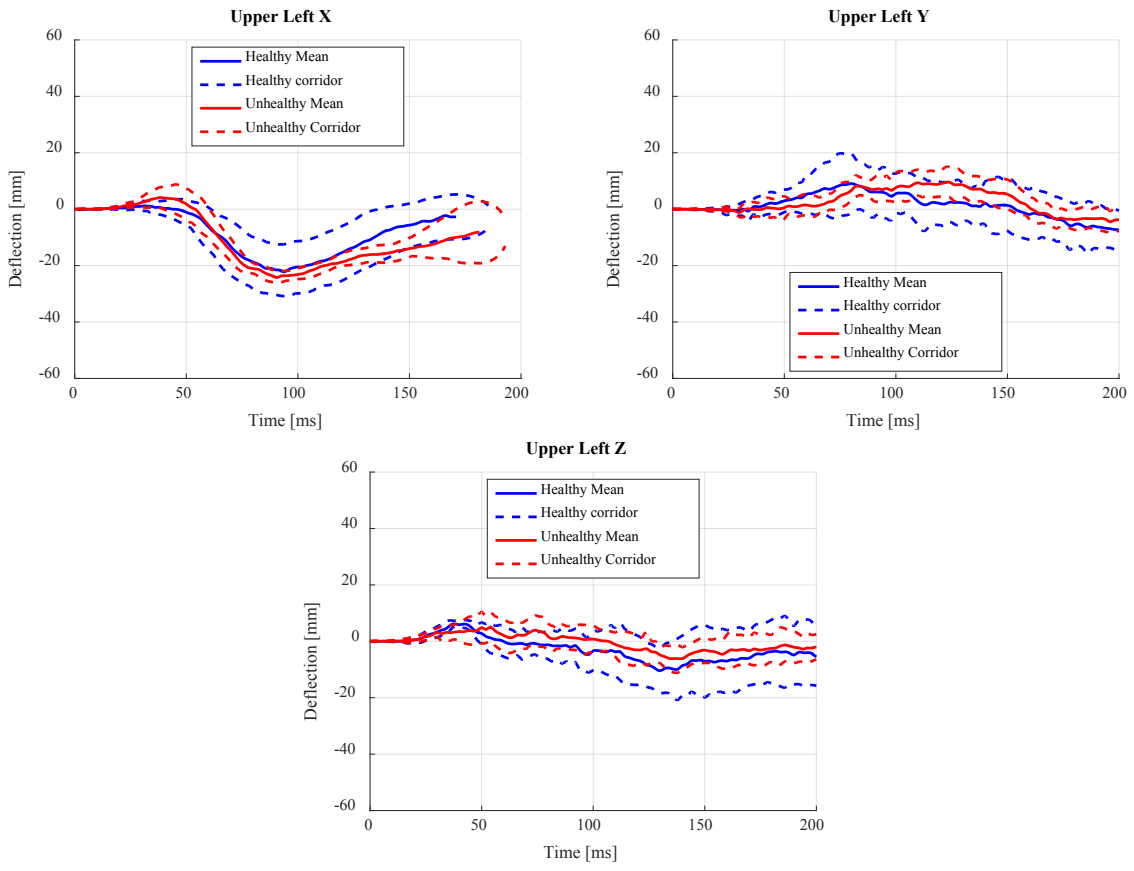


Figure 9. Thorax Upper Left deflection

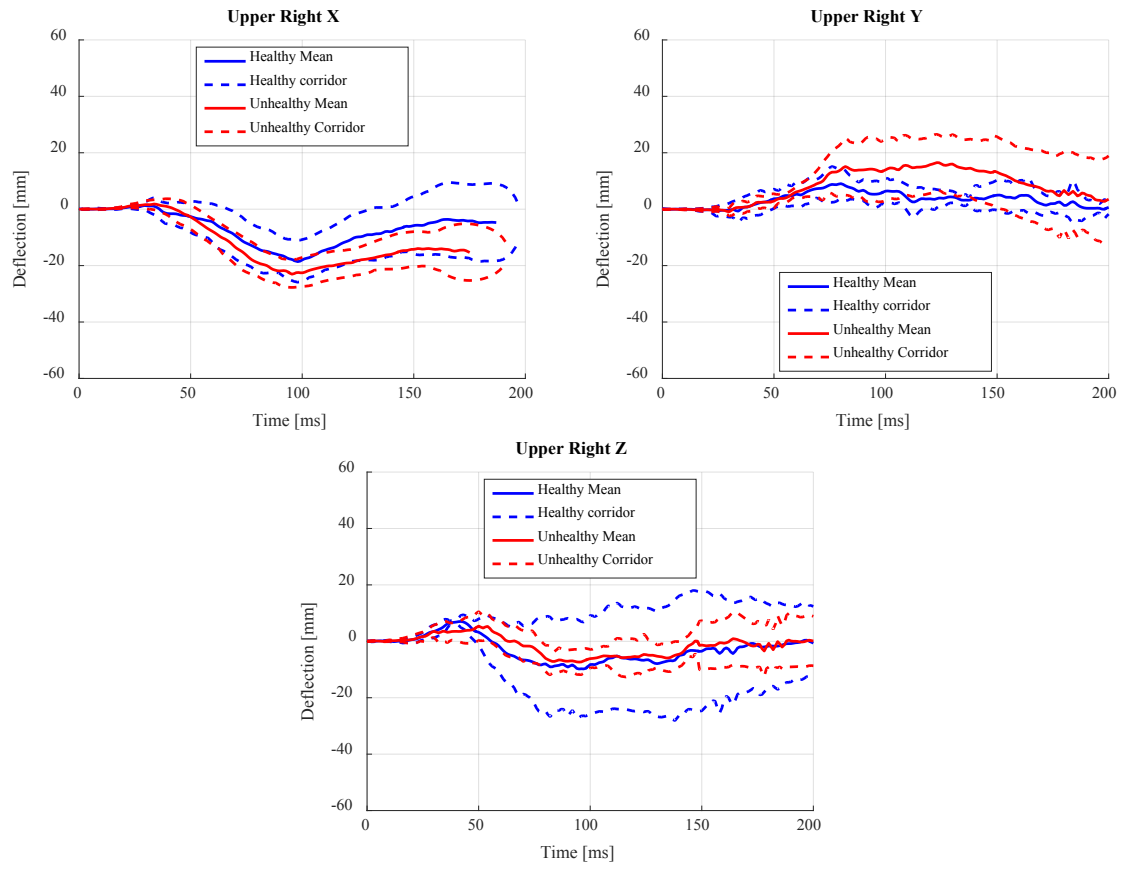


Figure 10. Thorax Upper Right deflection

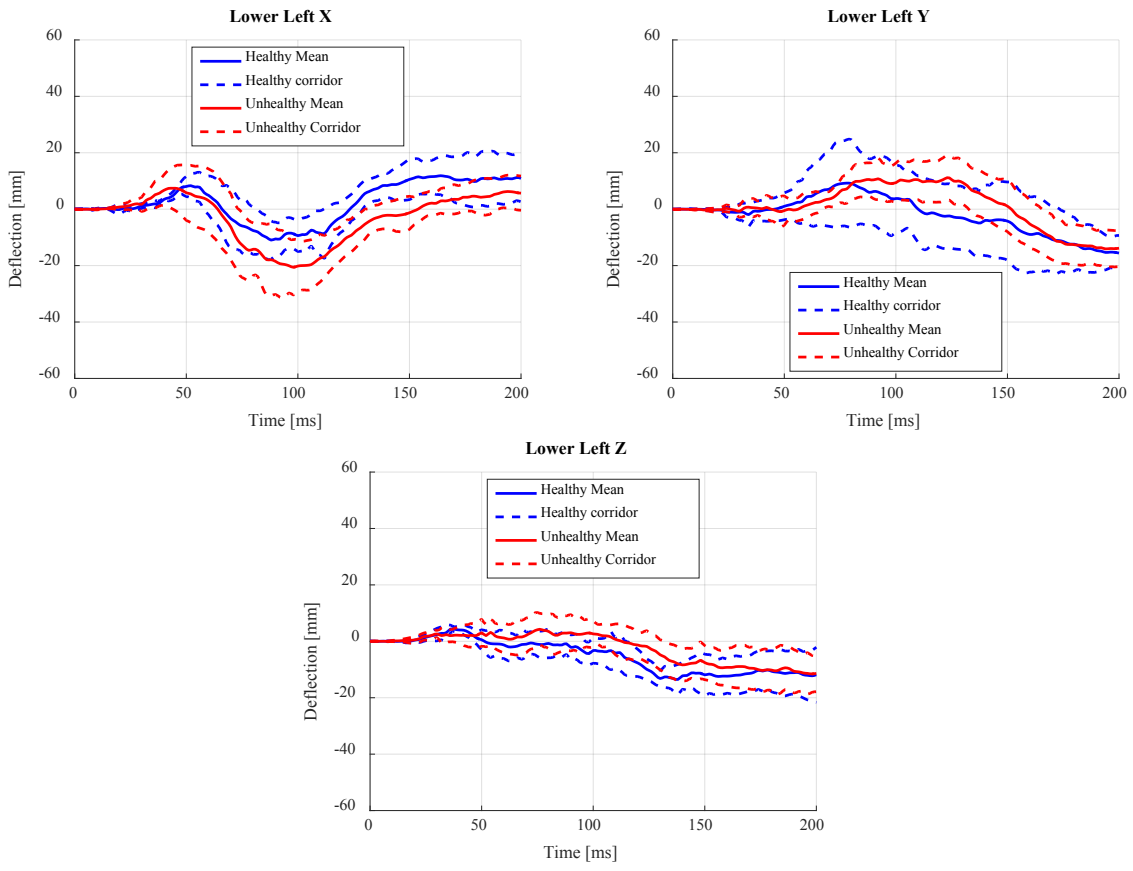


Figure 11. Thorax Lower Left deflection

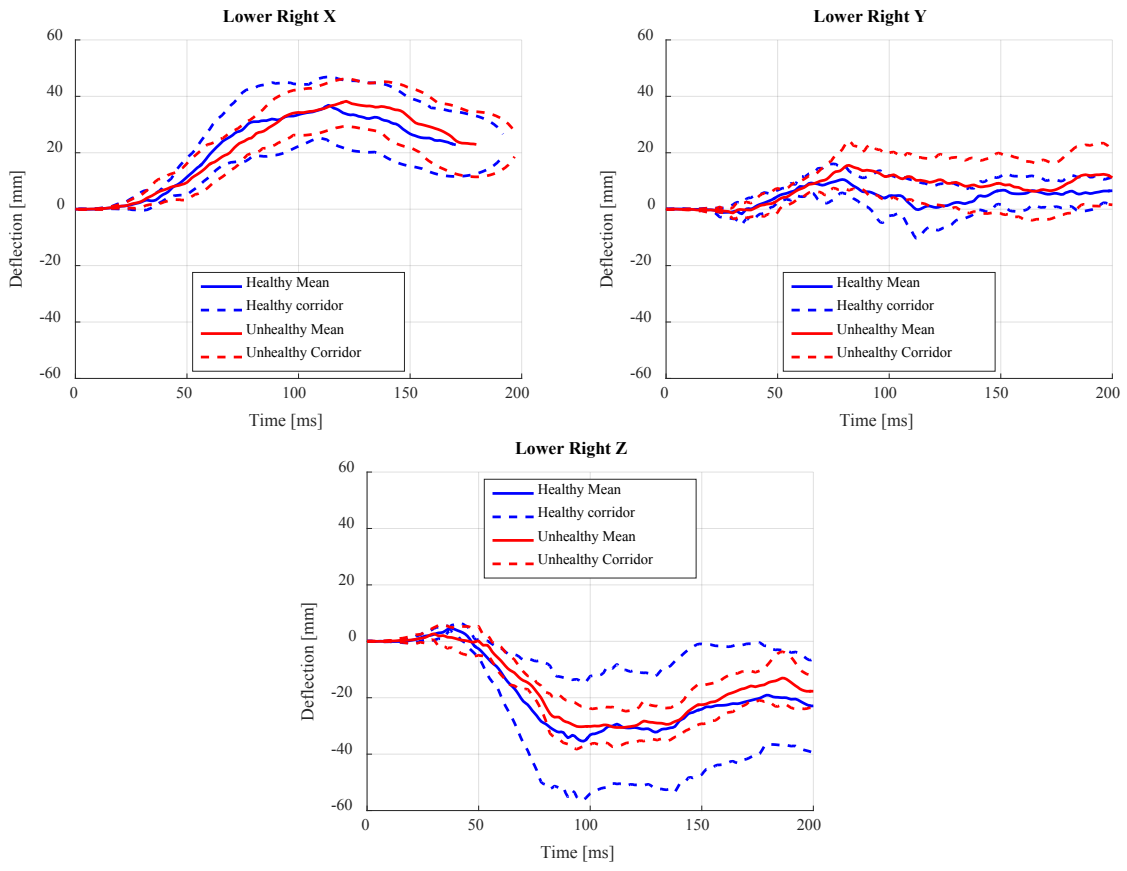


Figure 12. Thorax Lower Right deflection

Displacement of Anatomical centers

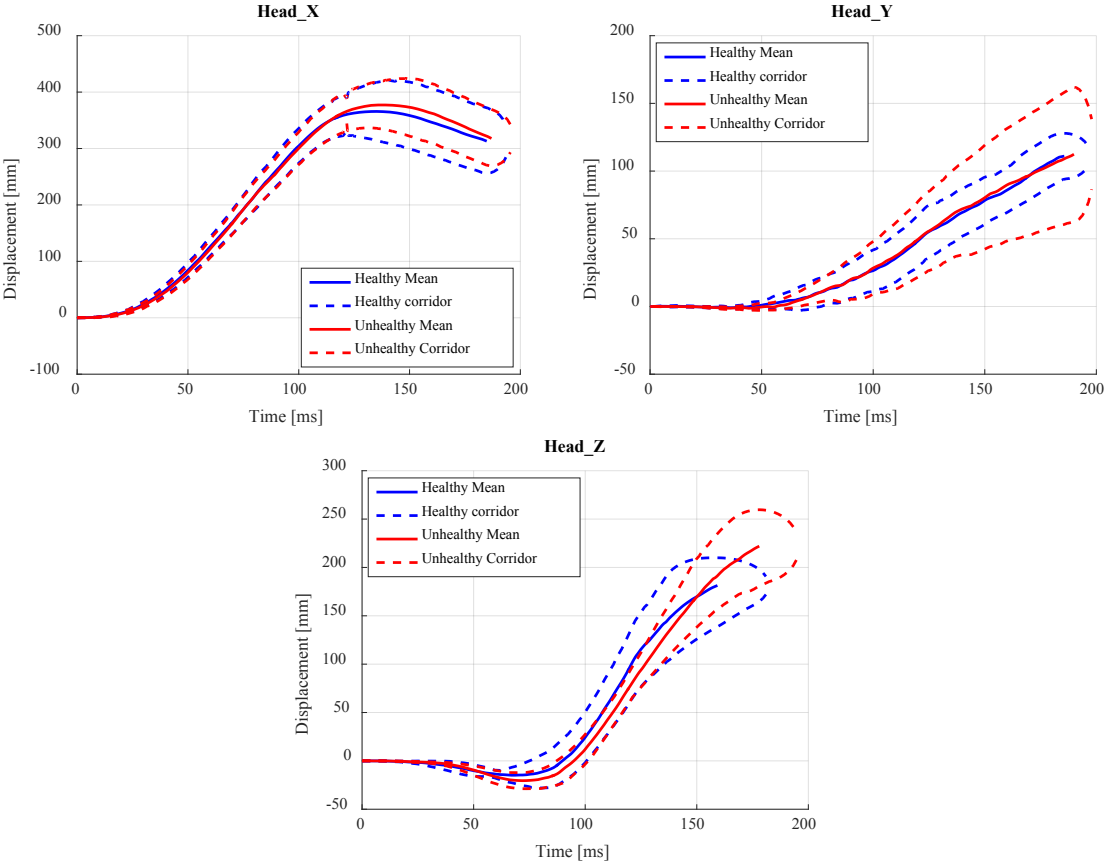


Figure 13. Head displacement

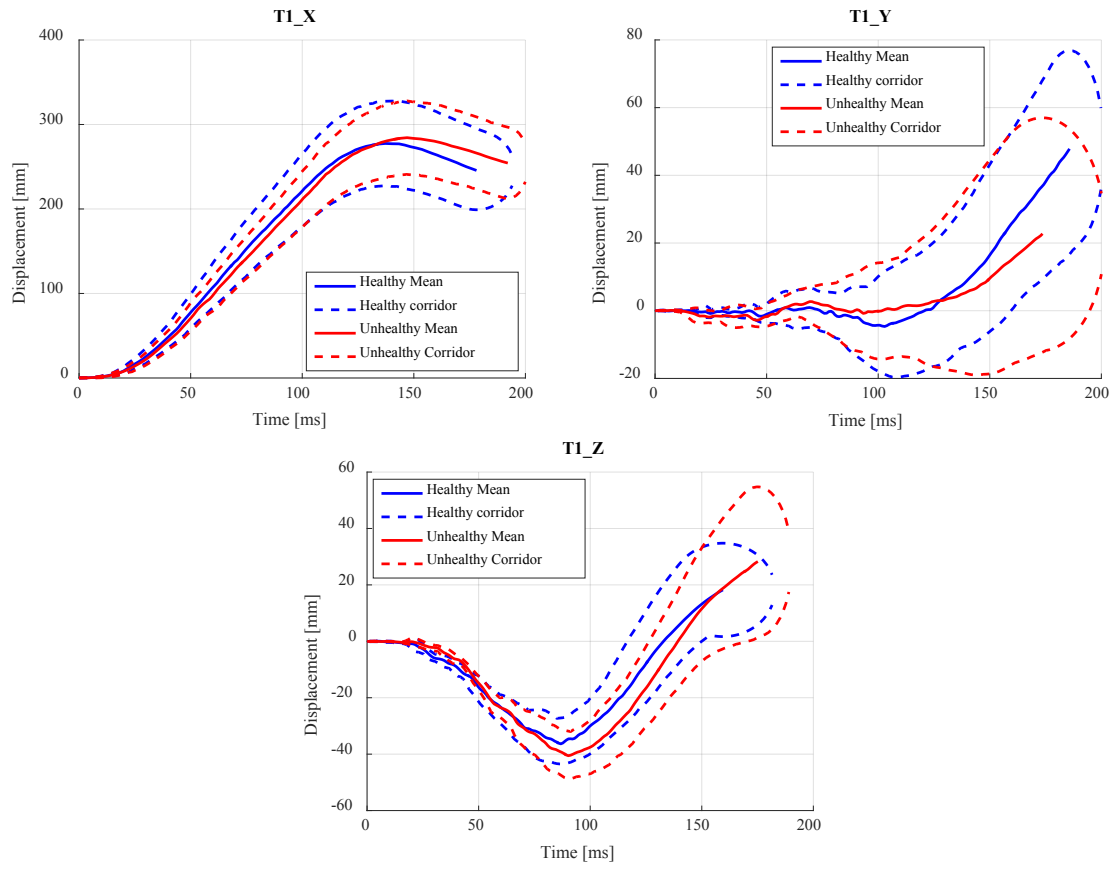


Figure 14. T1 displacement

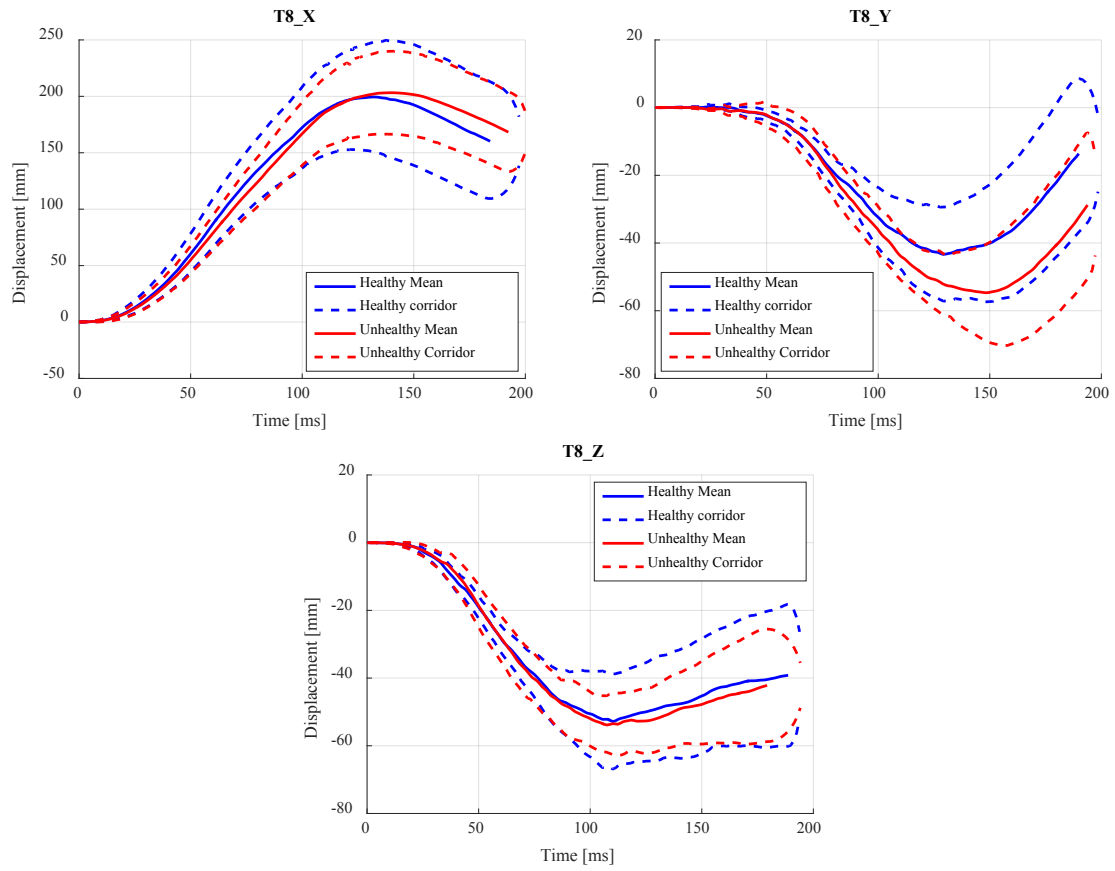


Figure 15. T8 displacement

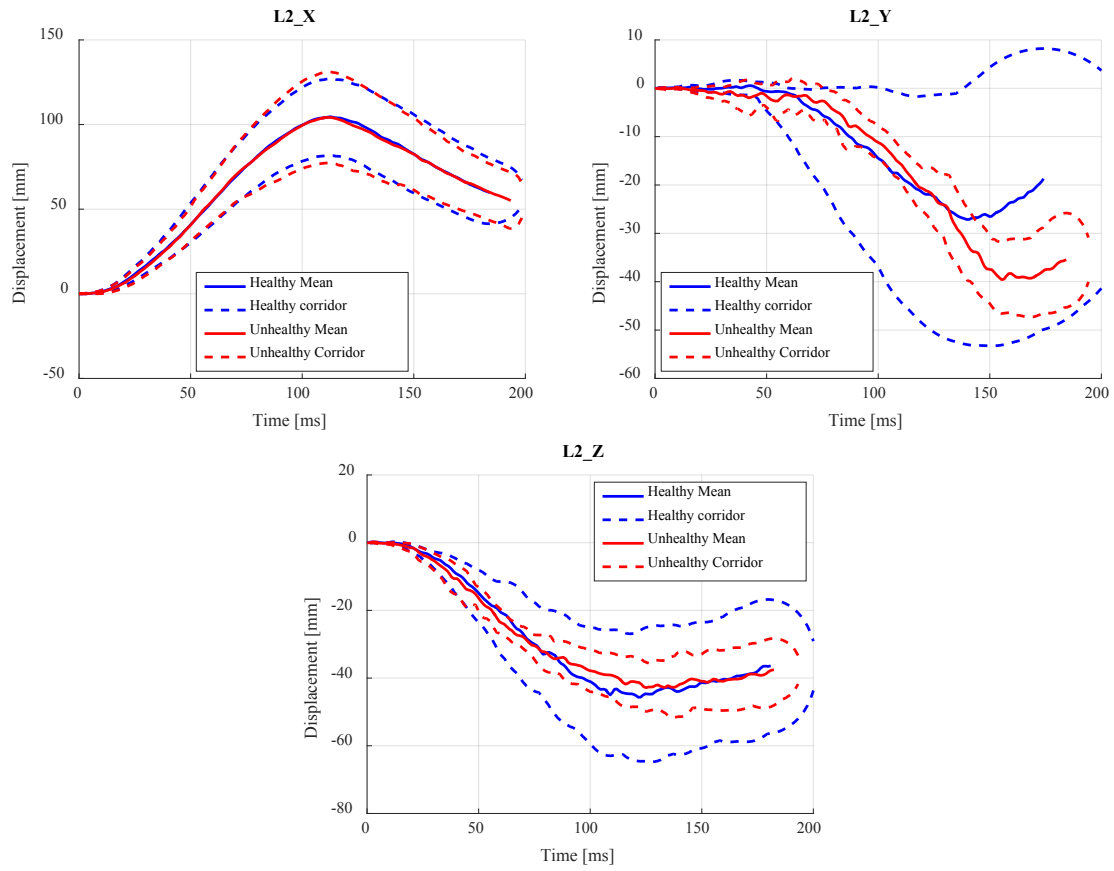


Figure 16. L2 displacement

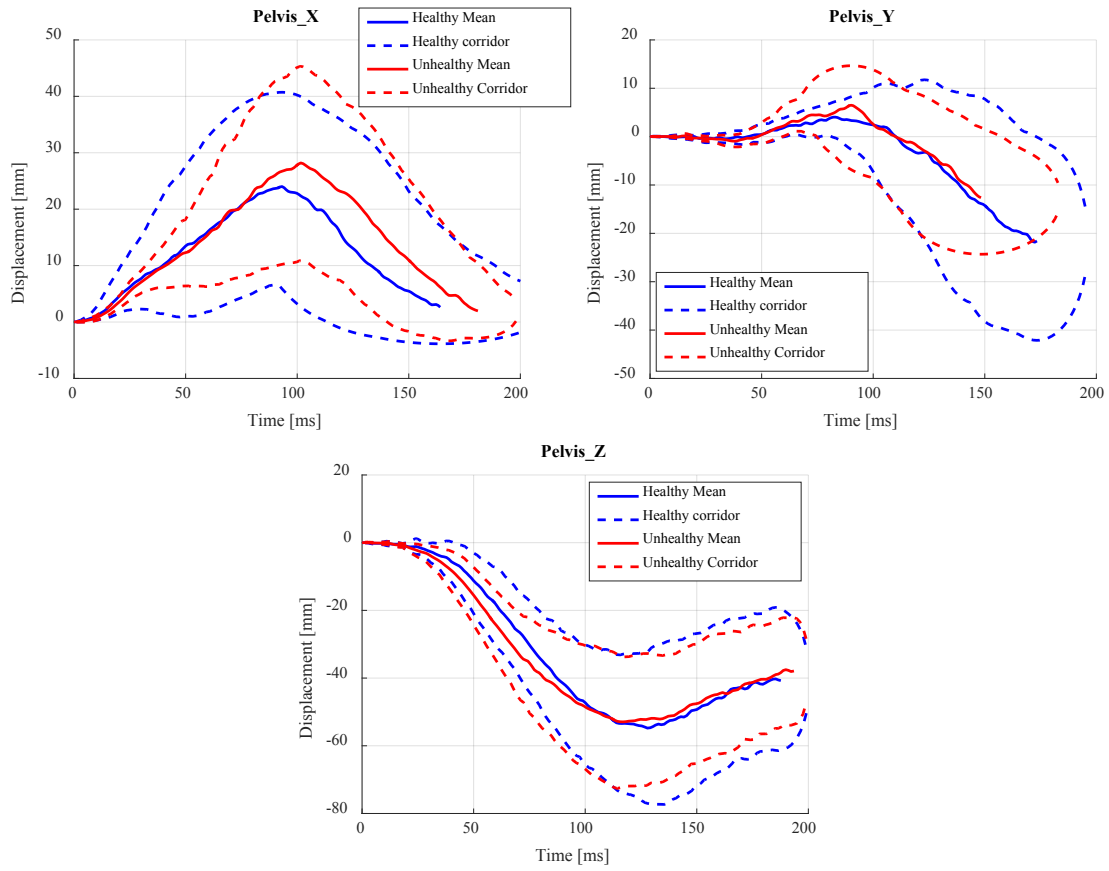


Figure 17. Pelvis displacement

Belt Forces

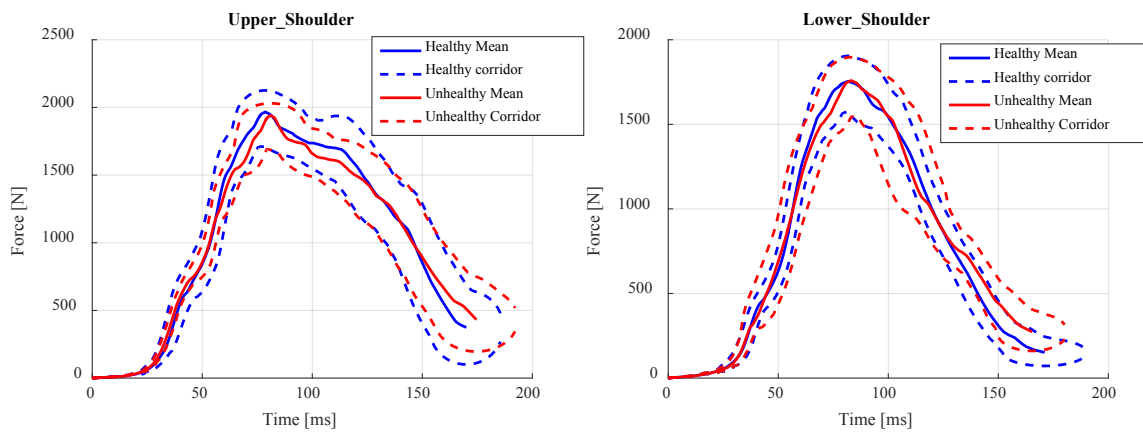


Figure 18. Shoulder Belt force

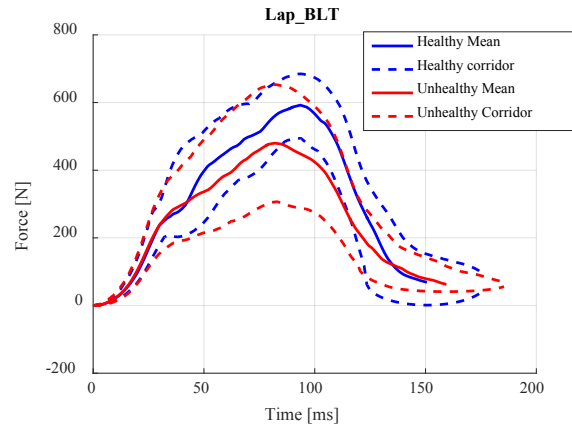


Figure 19. Lap belt force

Buck Load Cell

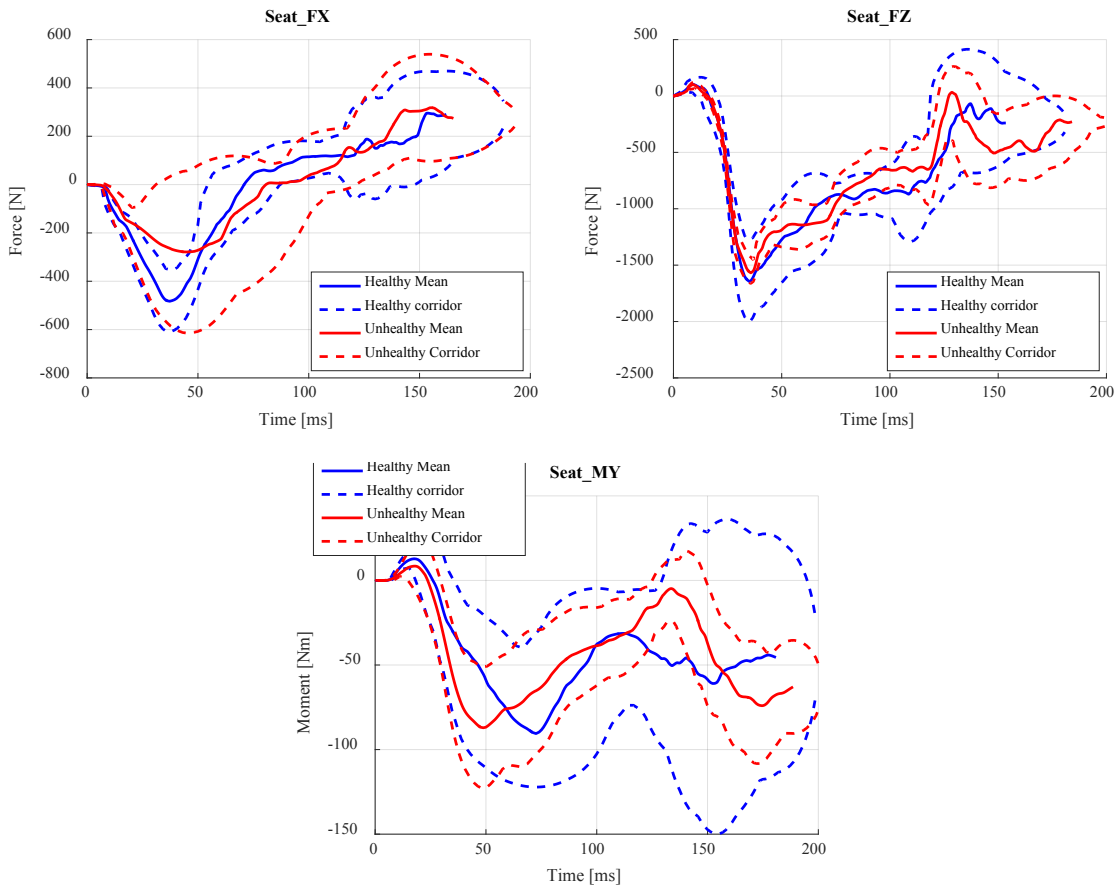


Figure 20. Seat load cell

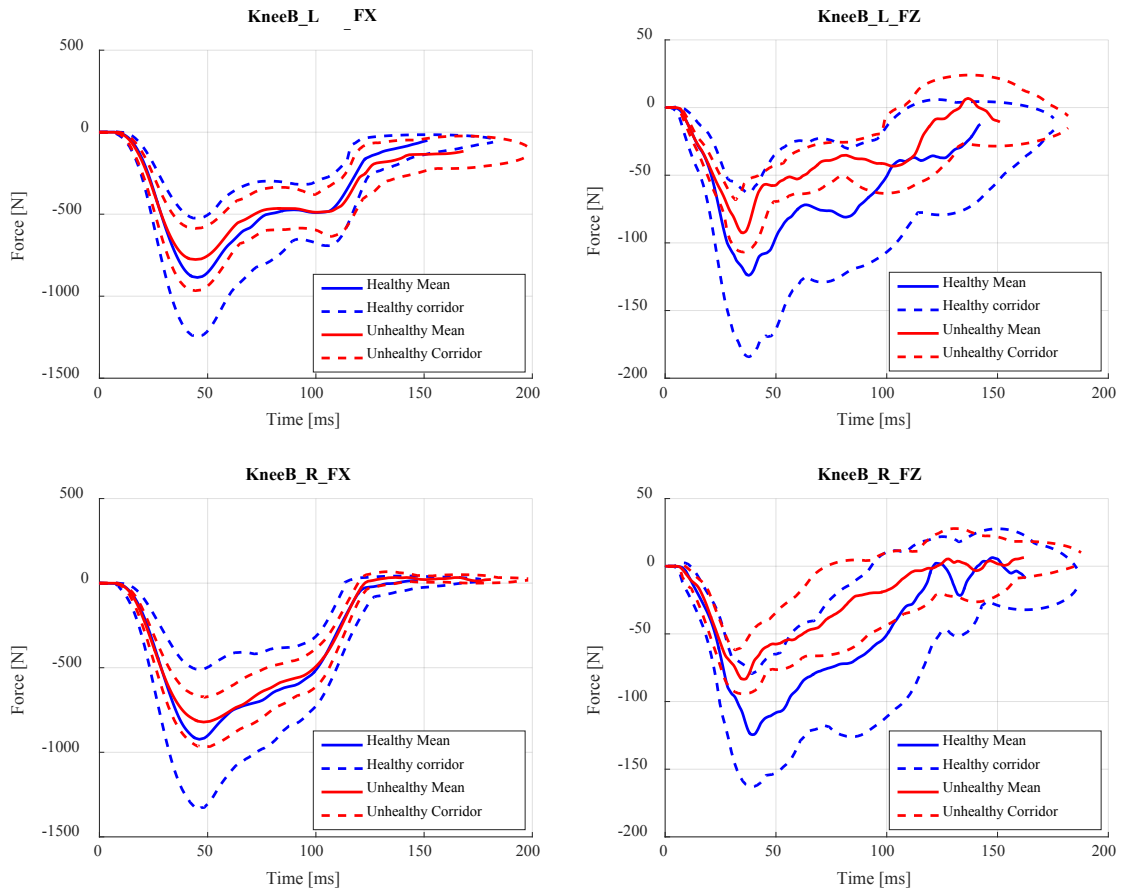


Figure 21. Knee bolster load cells

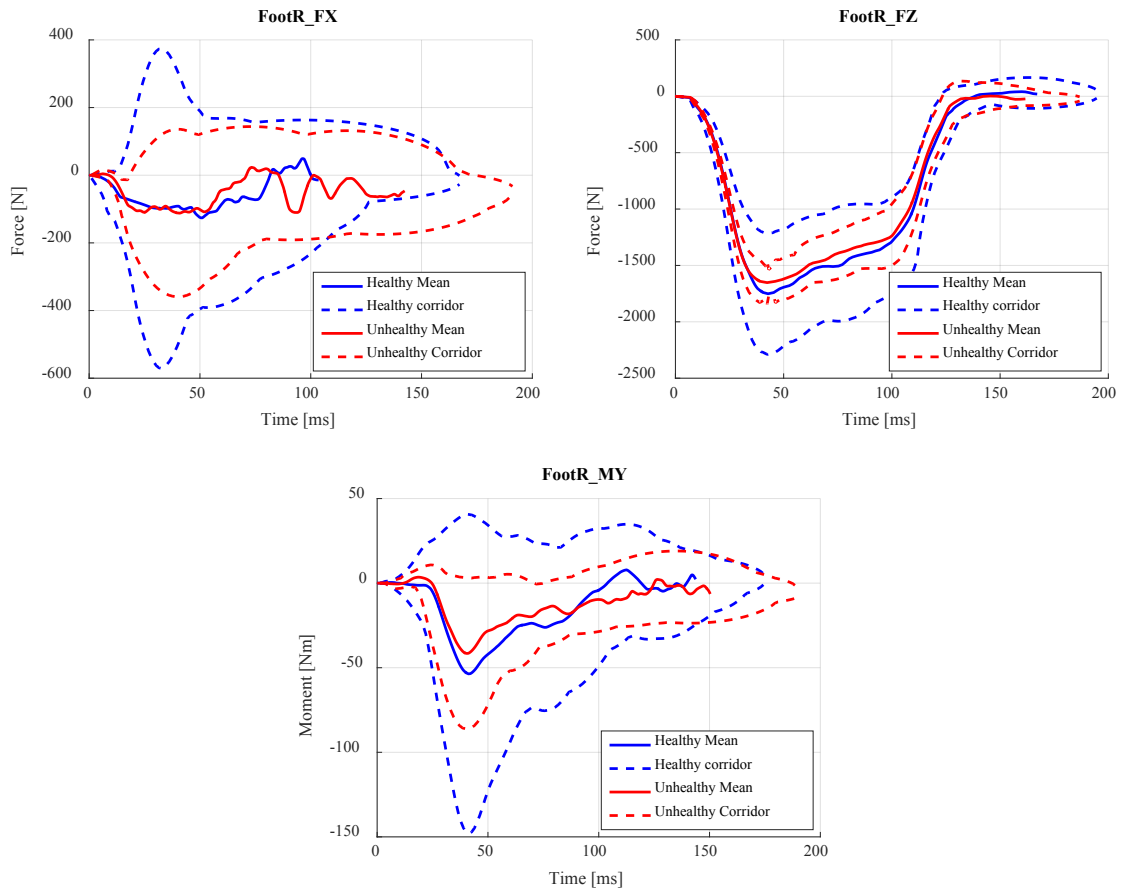


Figure 22. Foot rest load cell

Angular rate

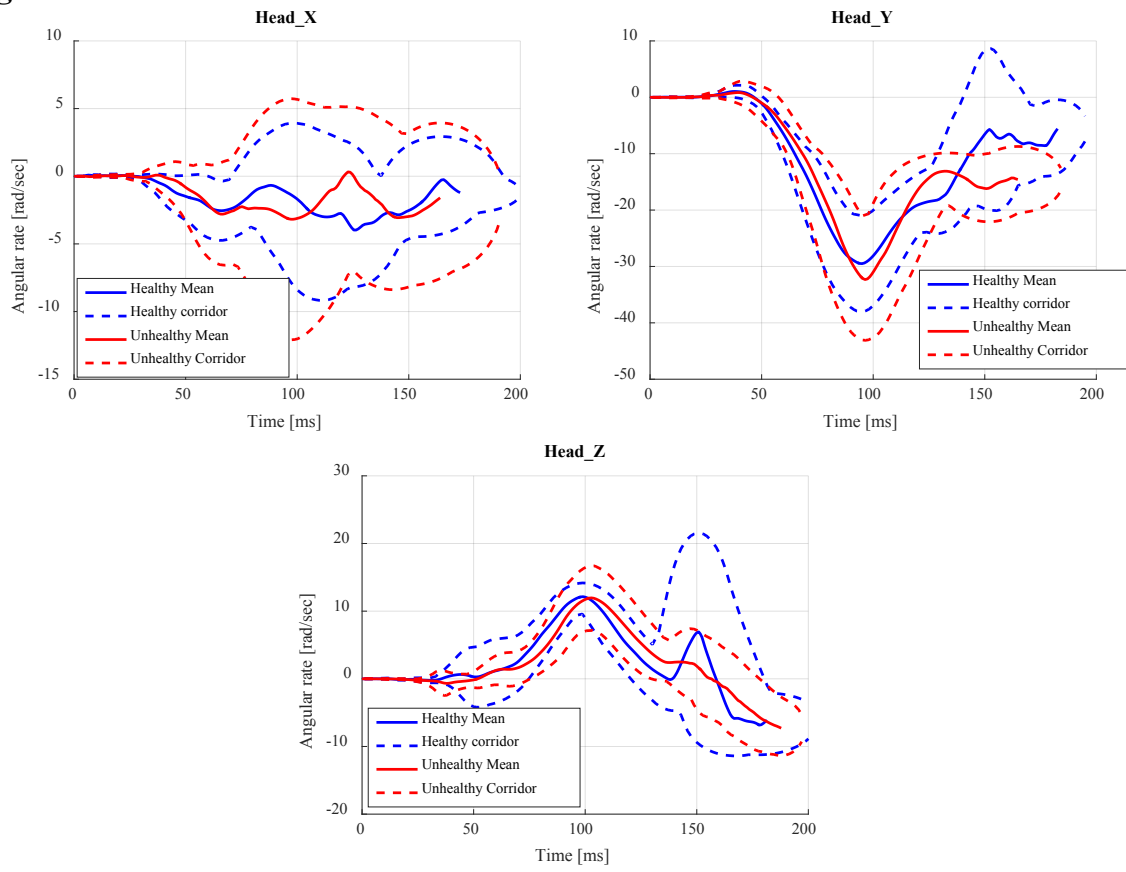


Figure 23. Head angular rate

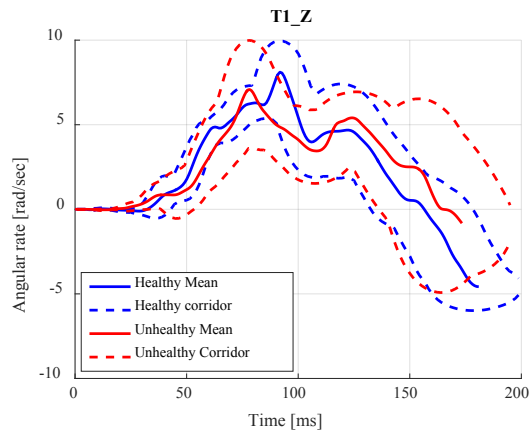
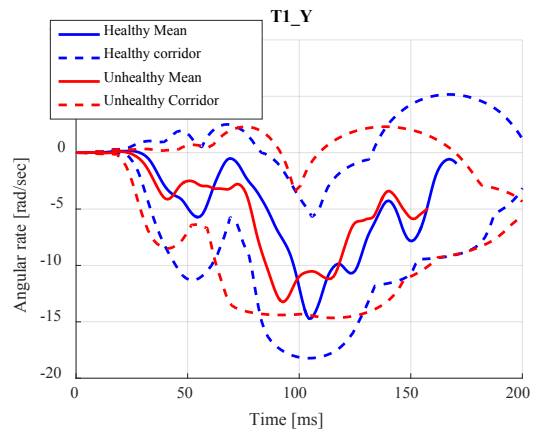
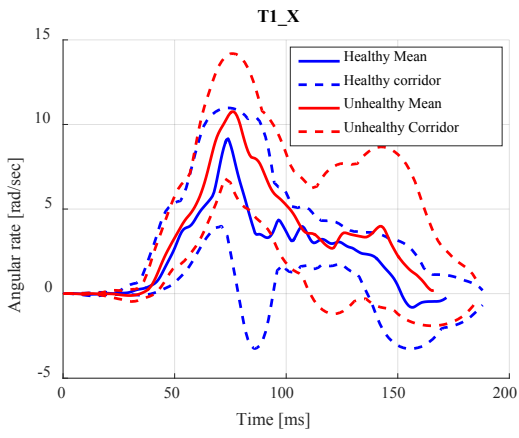


Figure 24. T1 angular rate

Acceleration

Test subjects S0212 (healthy) and S0372 (healthy) had large spikes in head acceleration signals (x & y direction) influencing the mean response of the rest of the group and therefore were excluded from the calculation of the head acceleration corridors.

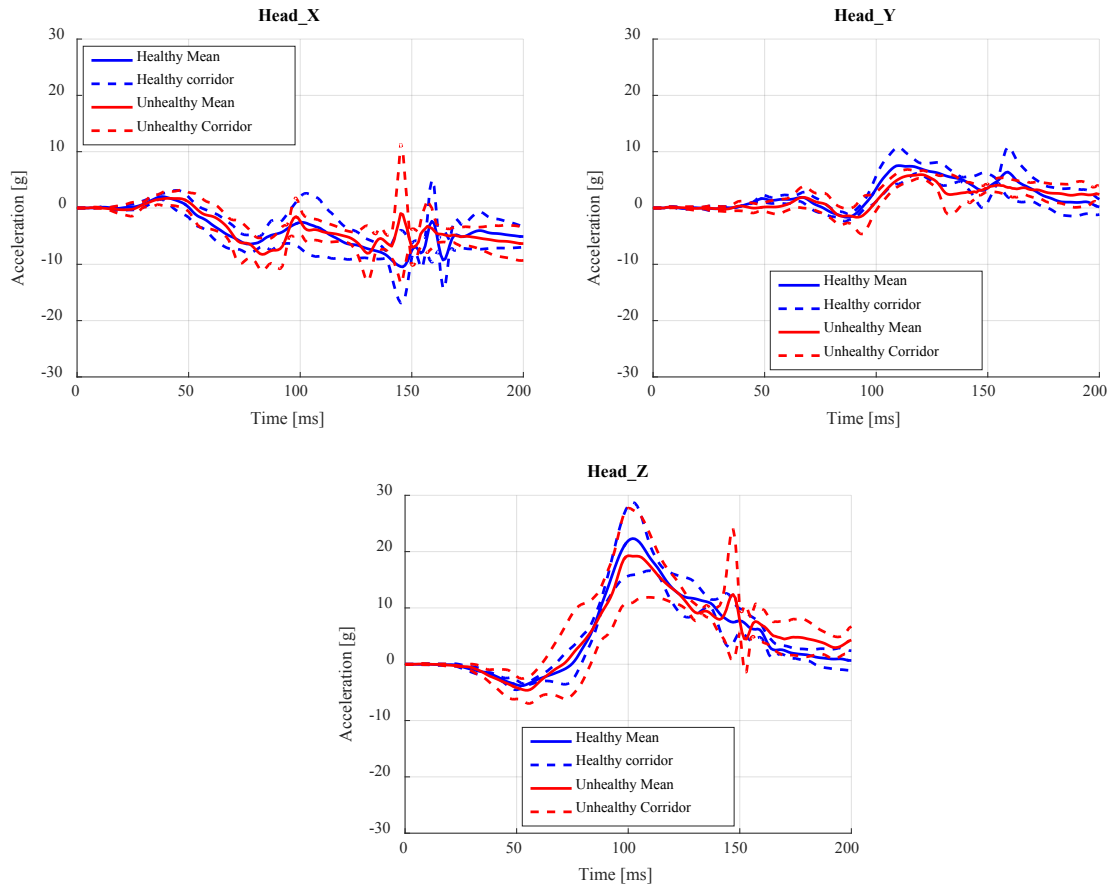


Figure 25. Head acceleration corridors

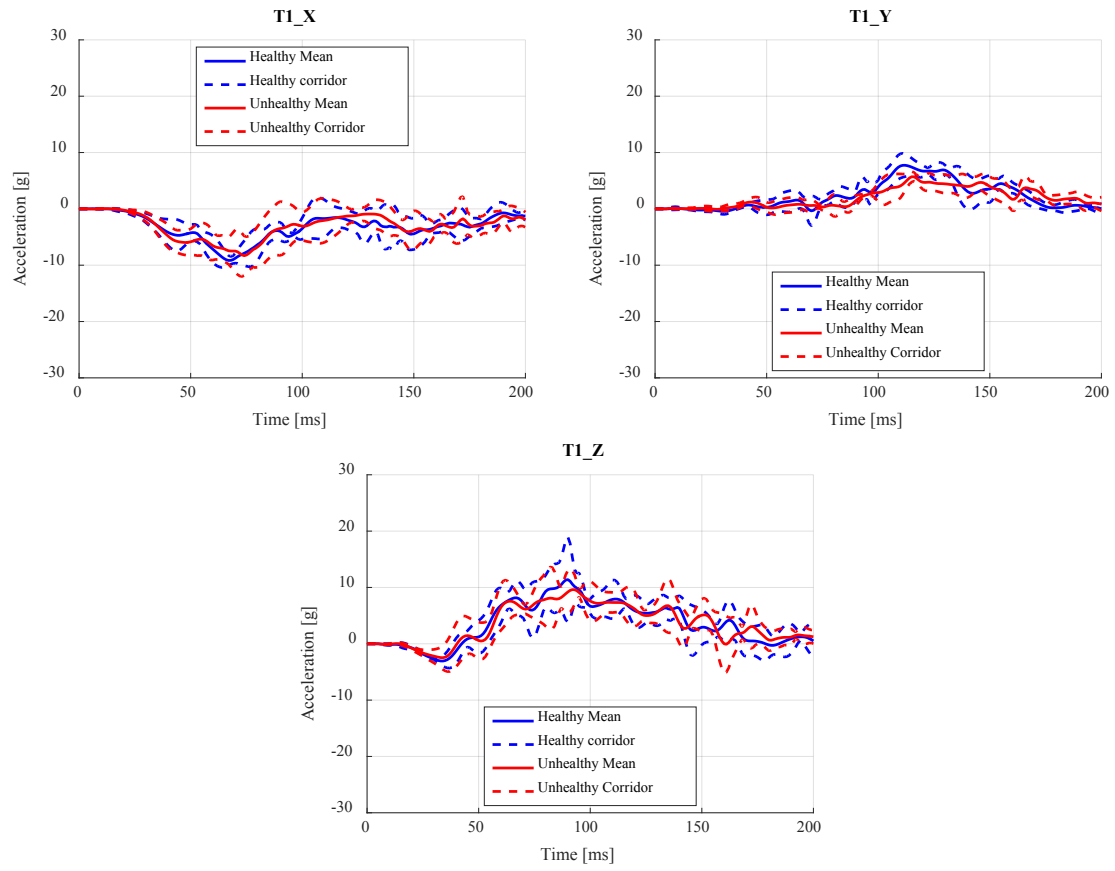


Figure 26. T1 acceleration corridors

Comparison of Healthy and Unhealthy Subjects

BioRank

Rhule, Maltese, Donnelly, Eppinger, Brunner, and Bolte (2002) developed the biofidelity rank (BioRank) metric to compare the response of dummies to human subject response. It involves the calculation of R that is the ratio of the cumulative variance between the dummy response and mean human response (DCV) over the cumulative variance between the mean human response and the mean plus one standard deviation (CCV) (Morgan, Marcus, & Eppinger, 1986). BioRank (\sqrt{R}) is defined as the square root of the ratio R. Following the procedure noted above we use the corridors developed from the healthy subjects to calculate the ratio R and BioRank (\sqrt{R}) for each of the unhealthy subjects, and then average the BioRank (\sqrt{R}) values for the compared signals.

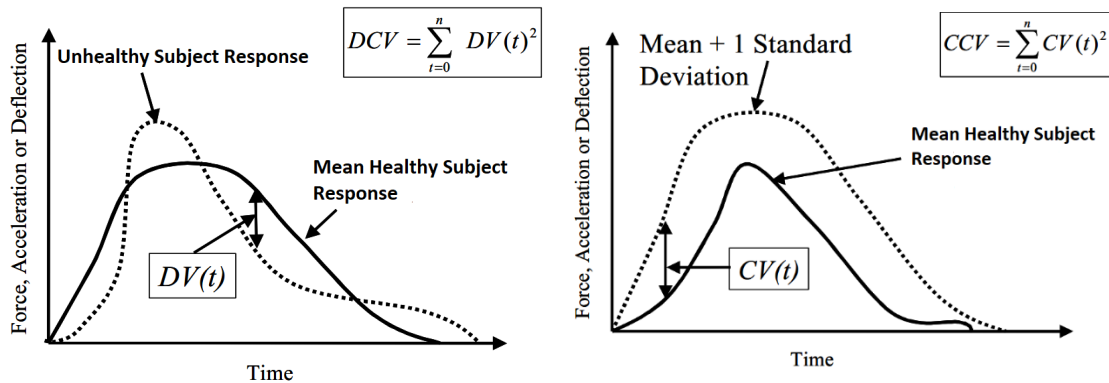


Figure 27. DCV and CCV (Bio Rank) adapted from Rhule et al.

A BioRank score of less than 1 indicates that the variation between the response of test group (unhealthy) and the control group (healthy) is less than the inherent variation present in the responses of the control group. Most of the responses, i.e., kinematics, chest deflection and belt forces, showed a BioRank of less than 1 (Table 3) or close to 1 indicating that the difference in responses of the healthy and unhealthy subjects was less than the inherent variation in responses observed among the healthy test subjects.

Table 3. Summary of BioRank evaluation

Signal	BioRank = \sqrt{R}
Upper Shoulder belt	0.49
Lower Shoulder belt	1.03
Lap Belt	1.16
Sternum	1.67
Chest Upper Left (X)	0.67
Chest Upper Right (X)	0.87
Chest Lower Left (X)	0.92
Chest Lower Right (X)	0.62
Head Displacement	0.74
T1 Displacement	0.75
T8 Displacement	0.65
L2 Displacement	0.91
Pelvis Displacement	0.67

Permutation Sampling test

A threshold of 1 was set to identify if the variation in the responses between the healthy and unhealthy subjects was less than the inherent variation in responses observed among the healthy subjects based on BioRank. However, it is difficult to justify a value for this ratio and draw conclusions about the statistical significance of the differences in the responses using BioRank. Based on an internal review, an alternate statistical approach was proposed to check for the statistical significance of the difference in the response corridors between the healthy and unhealthy subjects which is based on an approach called permutation sampling (Good, 2013). In this method we test the null hypothesis that there is no difference in the response corridors obtained from the sets of healthy and unhealthy subjects. The test statistic used to test this null hypothesis was the root mean squared error (RMSE) between the mean responses obtained from the healthy and unhealthy subjects. To estimate the sampling distribution of the test statistic we need many samples generated under the null hypothesis. When the null hypothesis holds true there is no difference in the way you select the two groups of healthy and unhealthy subjects for the corridor development. To test this, we randomly shuffled the ten subjects and selected 5 each time without repetition (Figure 28) into the healthy group and placed the rest into unhealthy group. A total number of $^{10}C_5$ combinations are presented to us which results in 252 virtual samples of healthy and unhealthy groups. The RMSE_i for each such virtual sample is calculated and the distribution of RMSE_i for the entire population of 252 virtual samples is then populated for a response characteristic (Figure 29). The p-value for a response characteristic was calculated as the proportion of samples with RMSE_i greater than the RMSE_i observed in the original population of healthy and unhealthy subjects. The null hypothesis was accepted if the p-value was greater than the statistical significance level of 0.05.

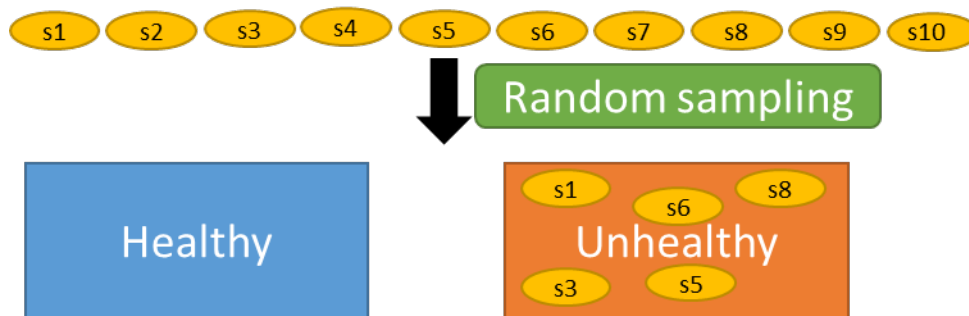


Figure 28. Random sampling of the subjects

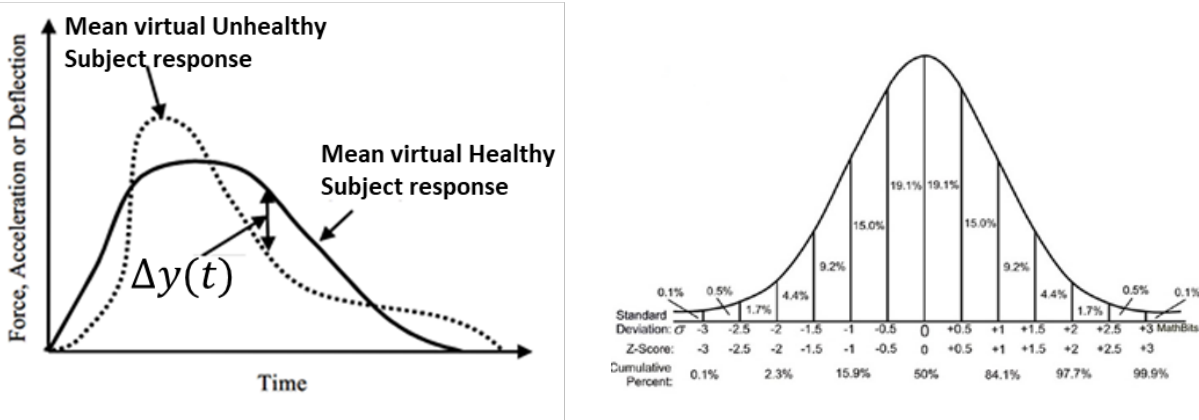


Figure 29. RMSEi estimation (left) and Distribution of RMSE (right)

For all the signals tested in the impact direction, except the sternum (X) deflection the null hypothesis can be accepted that there is no statistically significant difference in the responses of the healthy and unhealthy subjects with p-values >0.05 (Table 4). The sternum (X) deflection showed statistically significant difference with a p-value of 0.02 and therefore the sternum (X) deflection cannot be combined into a unified corridor. In the sternum (X) deflection, the unhealthy subjects exhibited a greater magnitude of deflection. This is consistent with the observation of a greater number of rib fractures in the unhealthy subjects, though the causal relationship between the two (whether the rib fractures resulted in greater deflection, or vice versa) is unknown.

Table 4. Summary of p-values from the permutation test

Signal	p-value
Upper Shoulder belt	0.76
Lower Shoulder belt	0.89
Lap Belt	0.30
Sternum (X)	0.02
Chest Upper Left (X)	0.32
Chest Upper Right (X)	0.12
Chest Lower Left (X)	0.27
Chest Lower Right (X)	0.63
Head Displacement	0.78
T1 Displacement	0.81
T8 Displacement	0.60
L1 Displacement	0.65
Pelvis Displacement	0.89

Unified response corridors

The data from healthy and un-healthy subjects were combined to create the ‘unified’ corridors for the signals that were not found to be significantly different between the healthy and unhealthy cohorts (Figure 30 - Figure 48). The deflection and displacement measurements in the nonimpact directions (Y and Z) and the angular rate signals were combined into unified corridors even though they were not checked for statistical difference. The Sternum corridors have been presented in the unified corridors section even though the healthy and unhealthy subjects showed statistically different response in the mean signals (Figure 8, Table 4).

Vicon Corridors

Thoracic Deflection

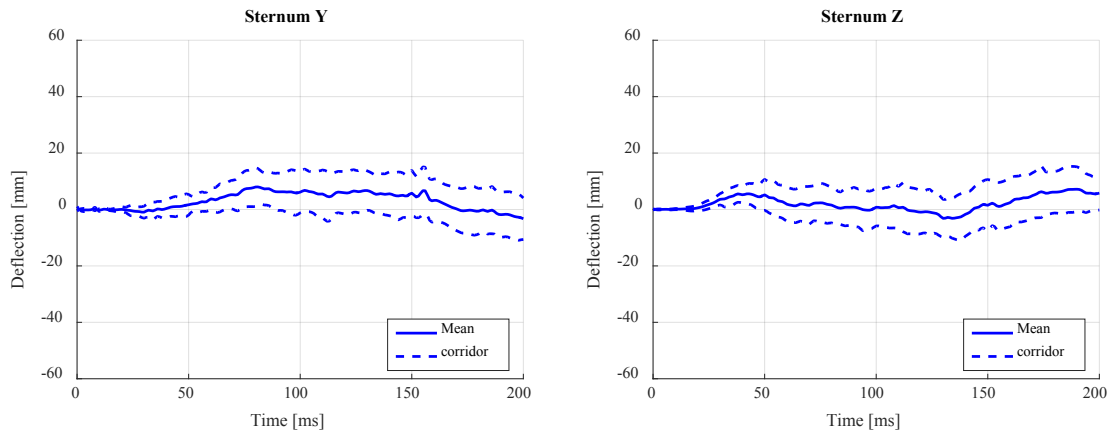


Figure 30. Sternum Y, and Z deflection (unified). [see Figure 8 for the Sternum X deflection]

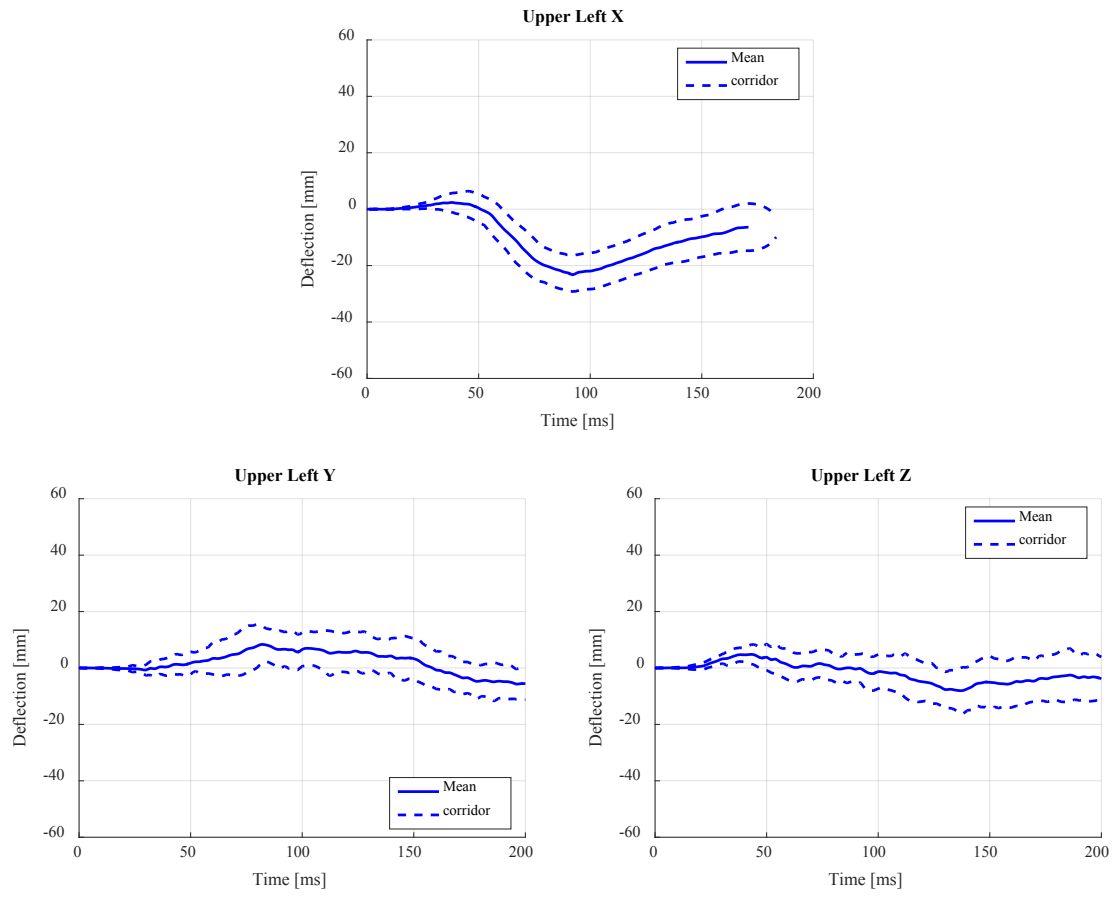


Figure 31. Left upper deflection (unified)

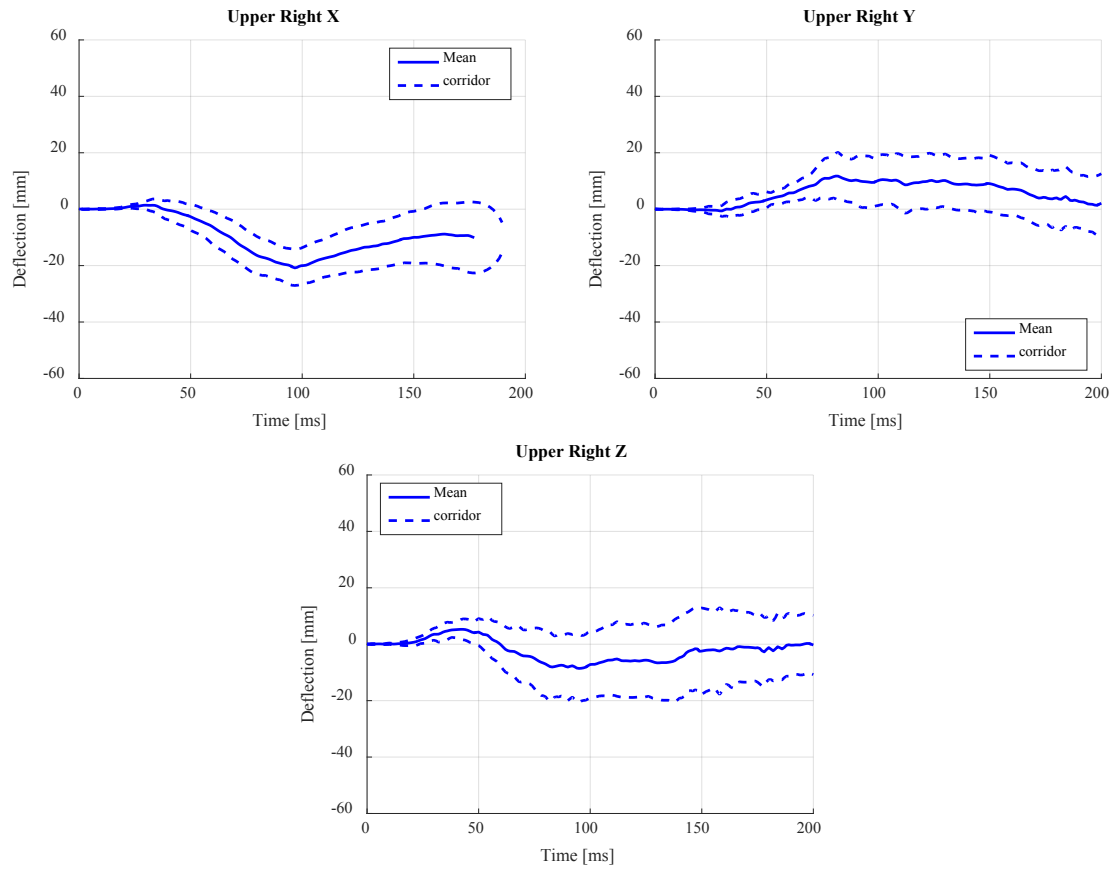


Figure 32. Right upper deflection (unified)

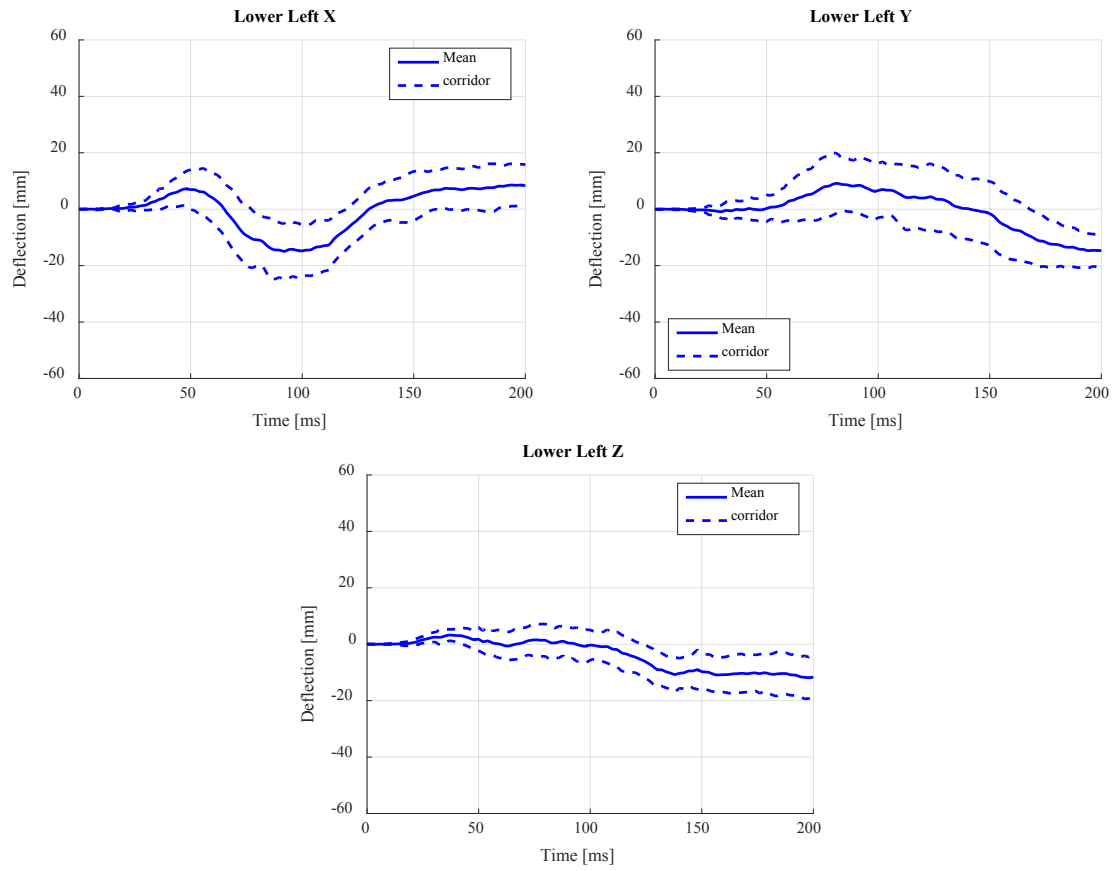


Figure 33. Left lower deflection (unified)

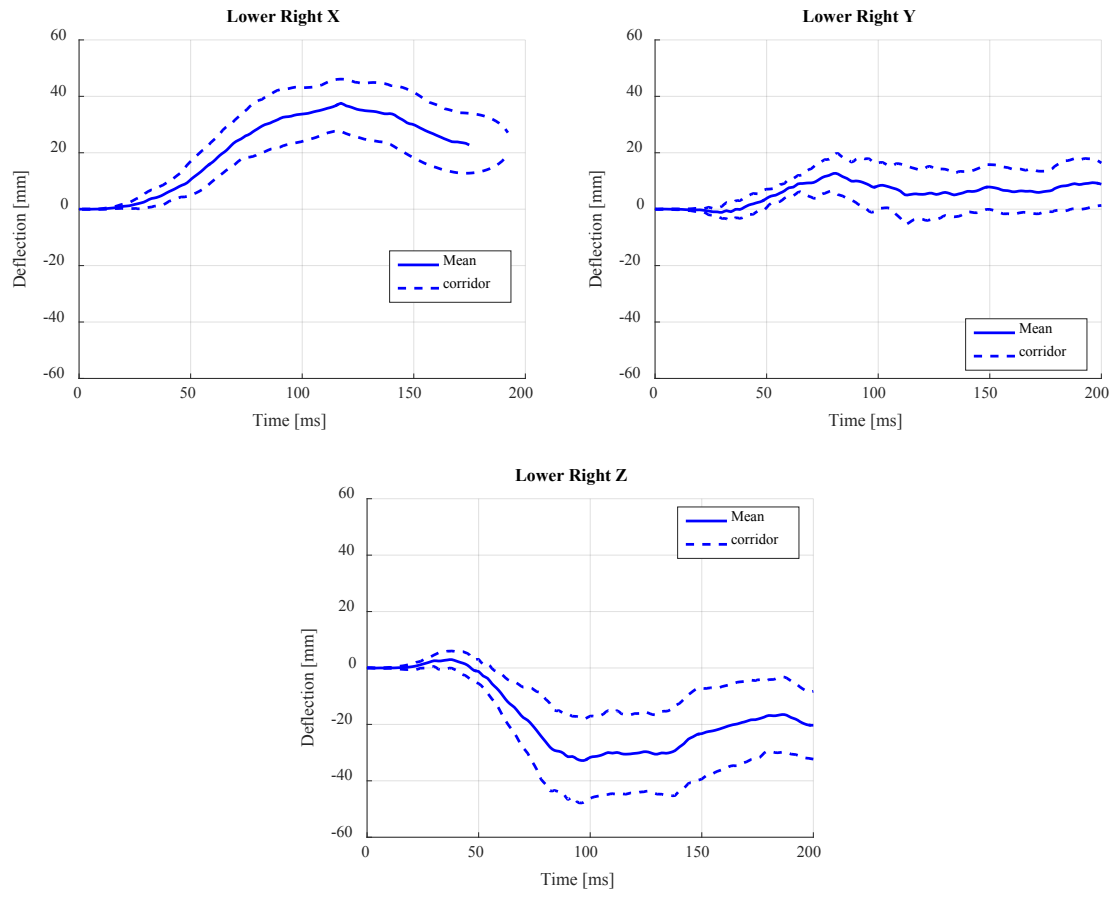


Figure 34 Right lower deflection (unified)

Displacement of Anatomical Centers

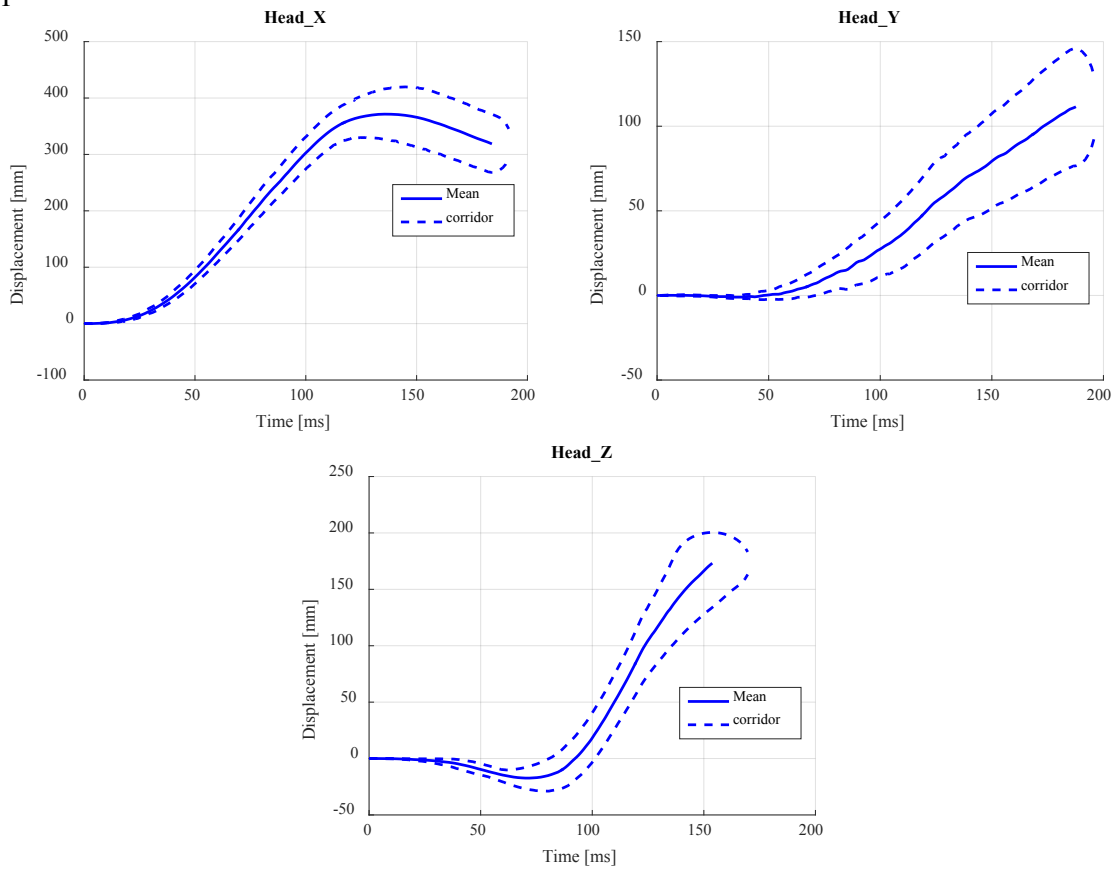


Figure 35. Head displacement (unified)

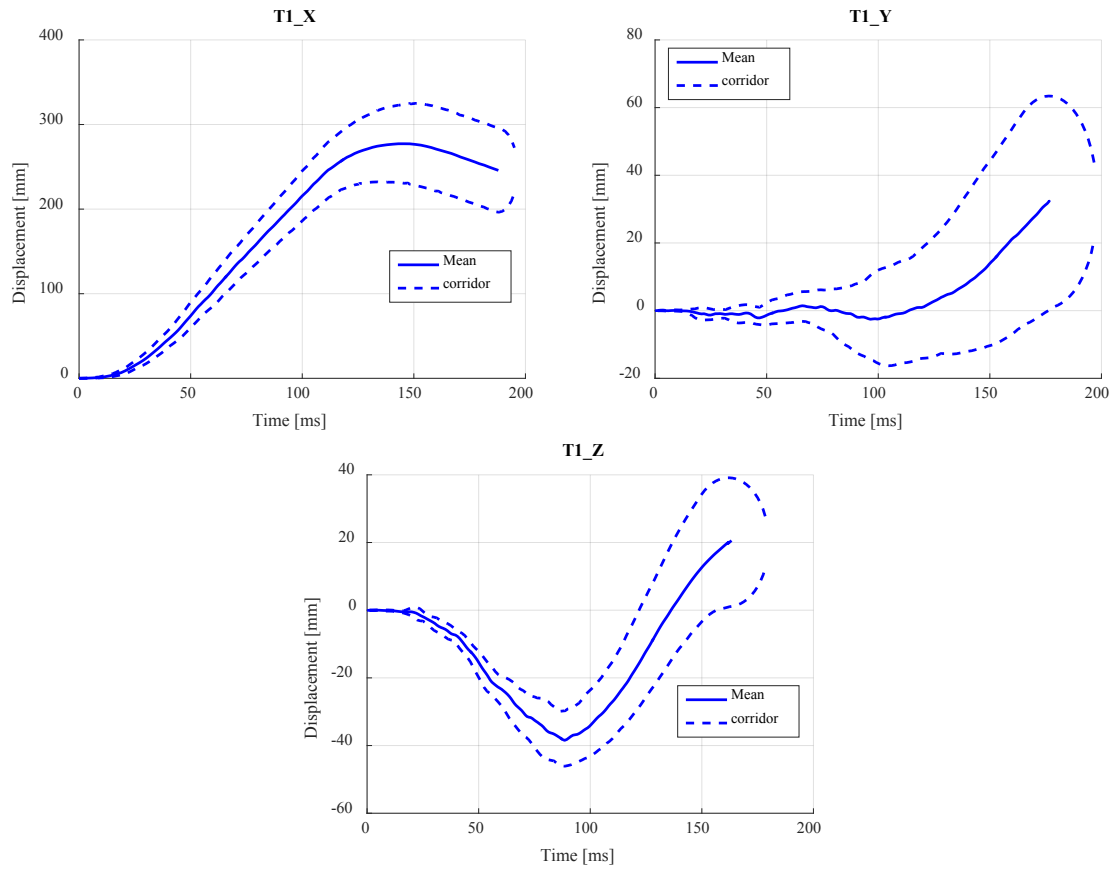


Figure 36. T1 displacement (unified)

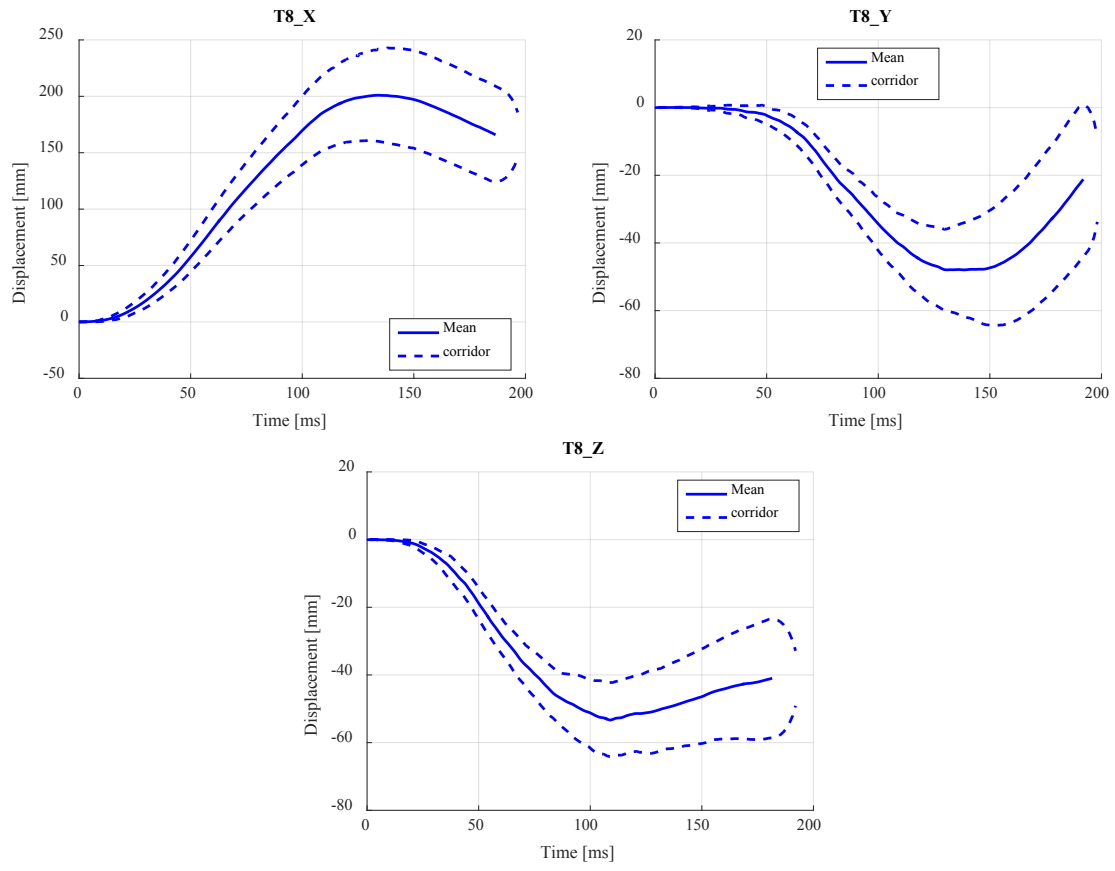


Figure 37. T8 displacement (unified)

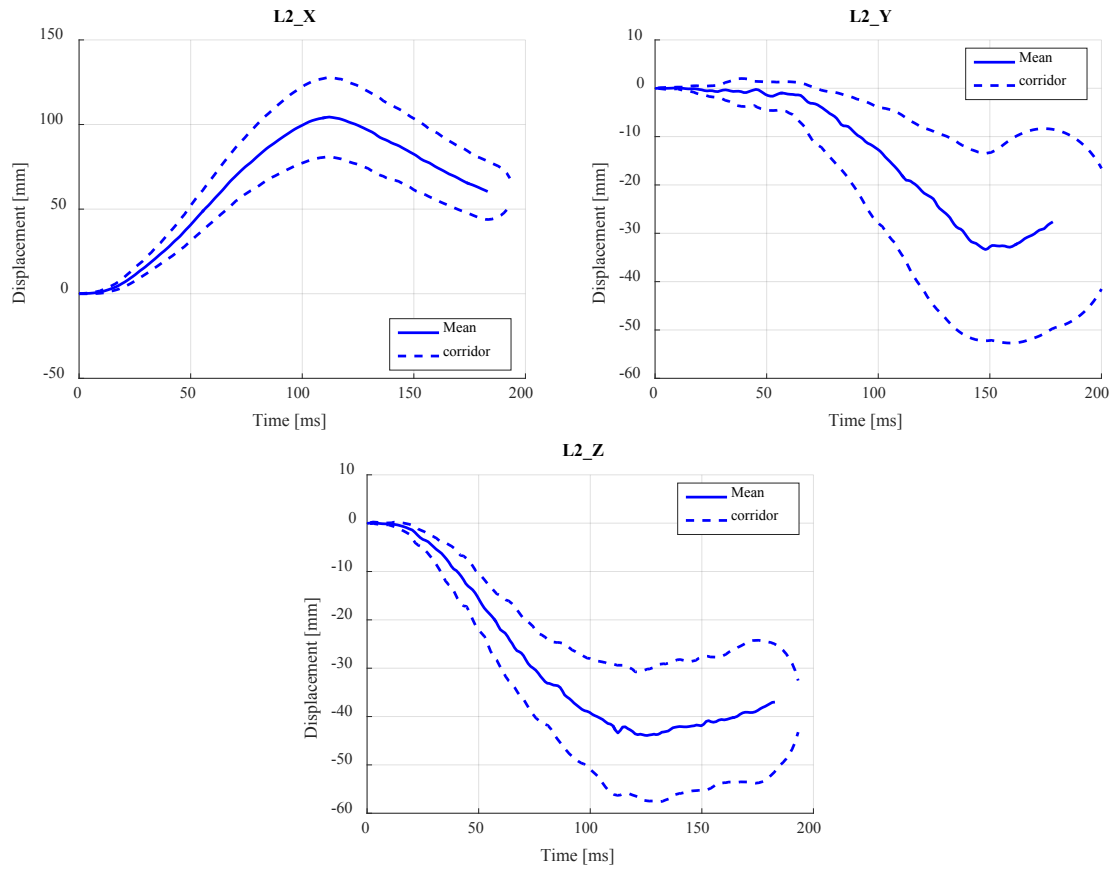


Figure 38. L2 displacement (unified)

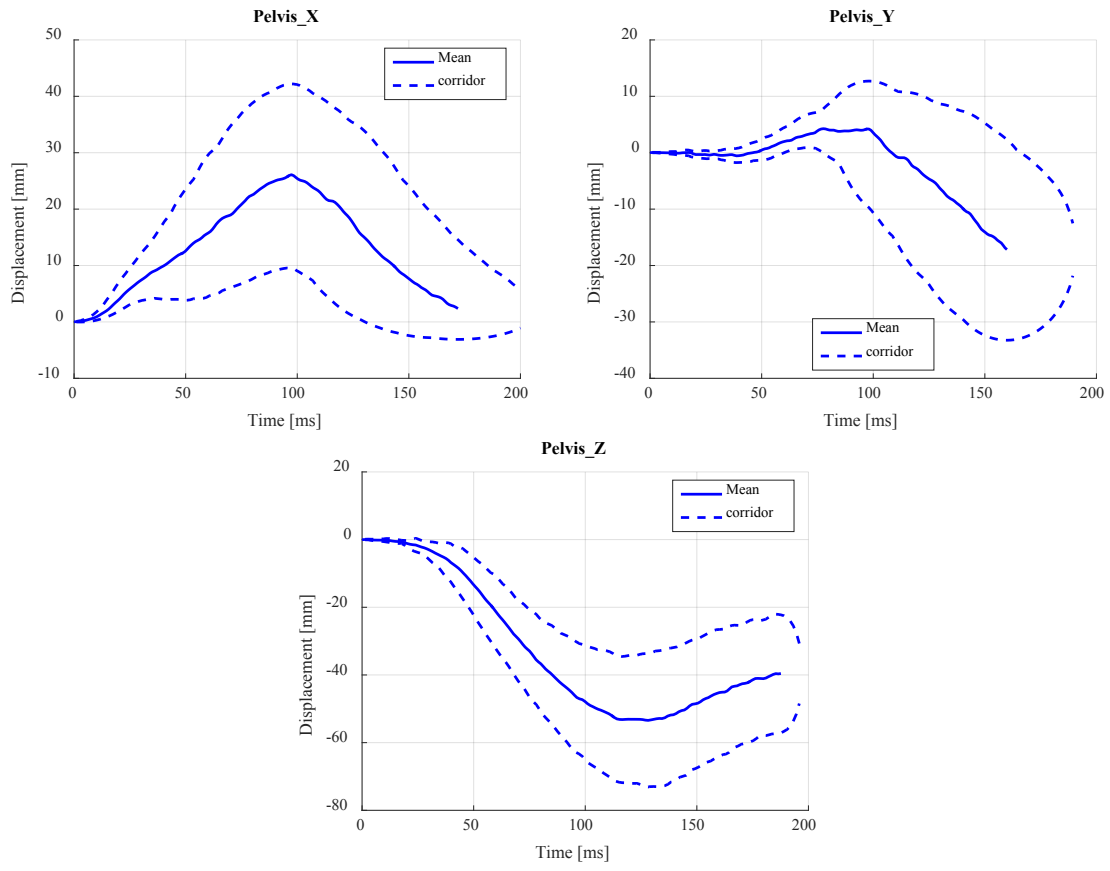


Figure 39. Pelvis displacement (unified)

Belt Forces

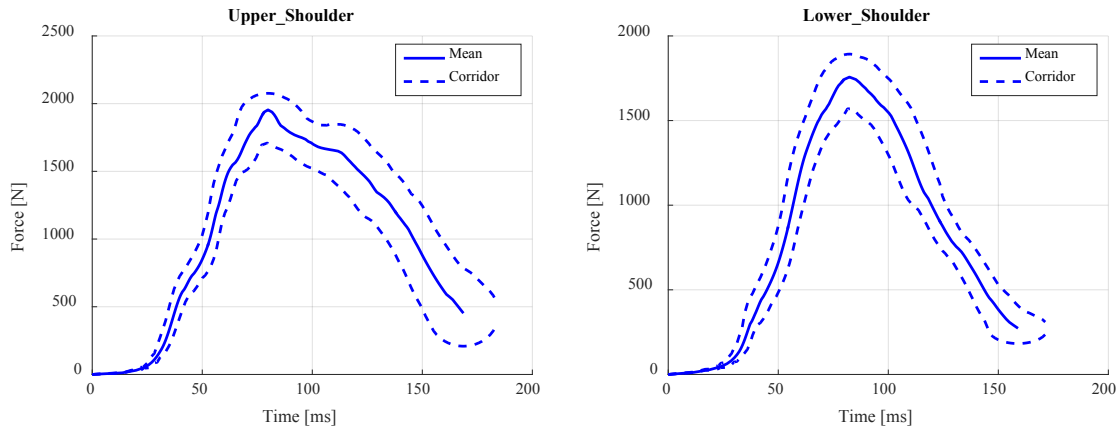


Figure 40. Shoulder belt force (unified)

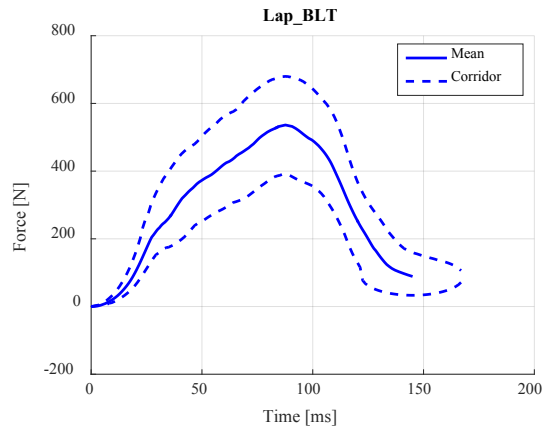


Figure 41. Lap belt force (unified)

Buck Load Cell

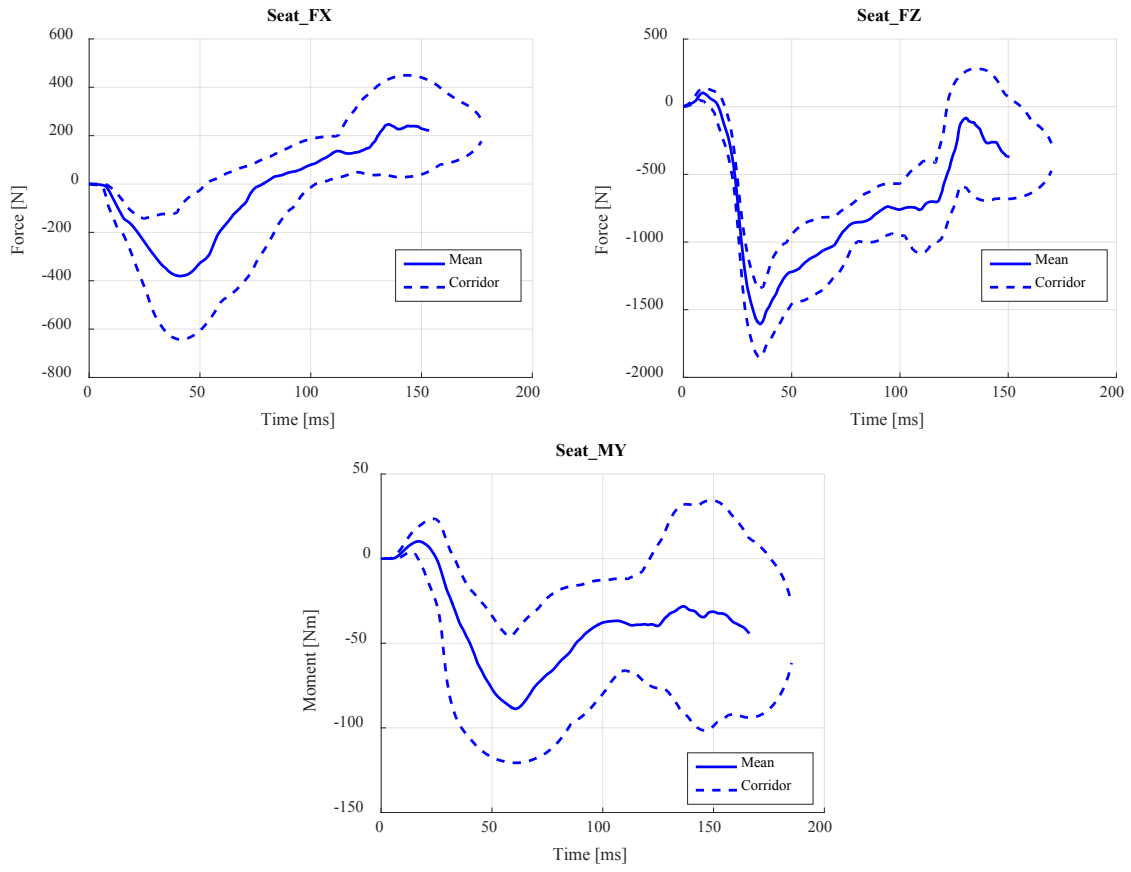


Figure 42. Seat load cell (unified)

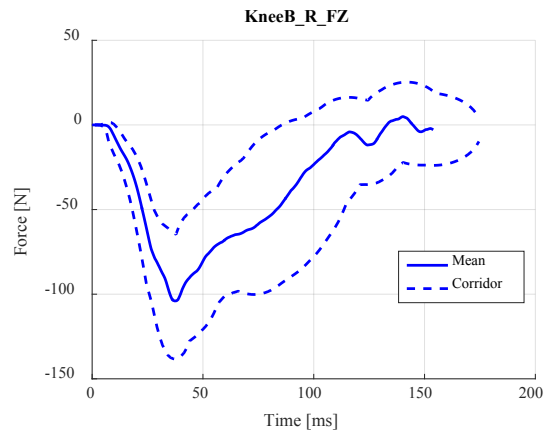
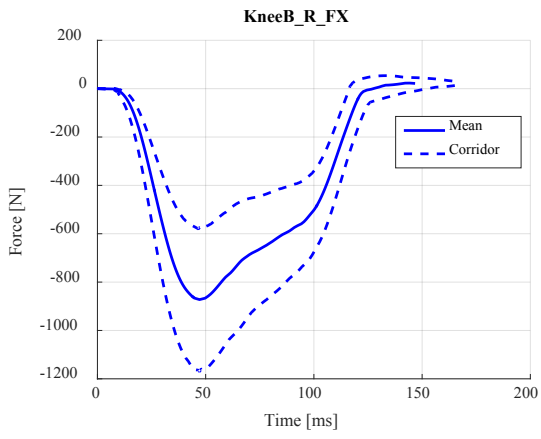
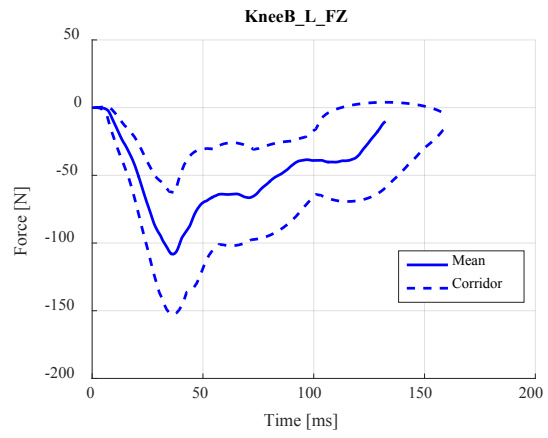
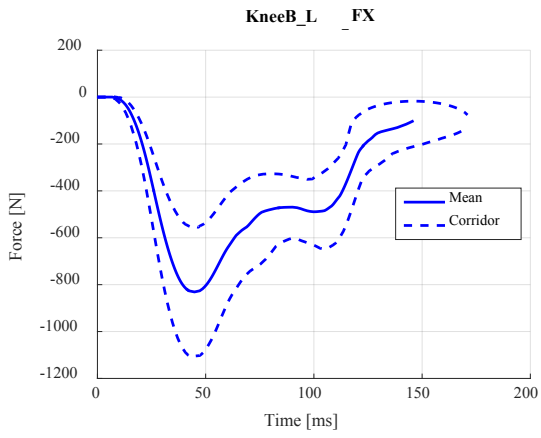


Figure 43. Knee bolster load cell (unified)

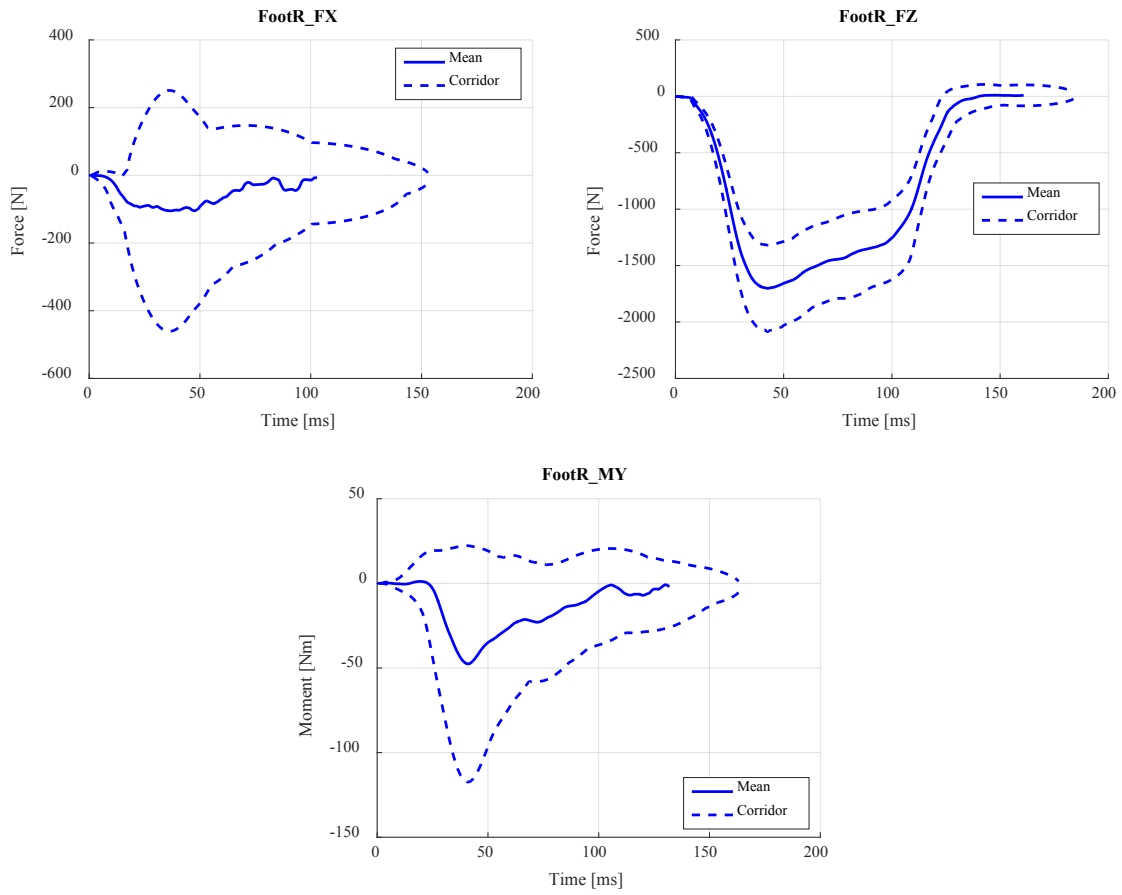


Figure 44. Foot rest load cell (unified)

Angular rate

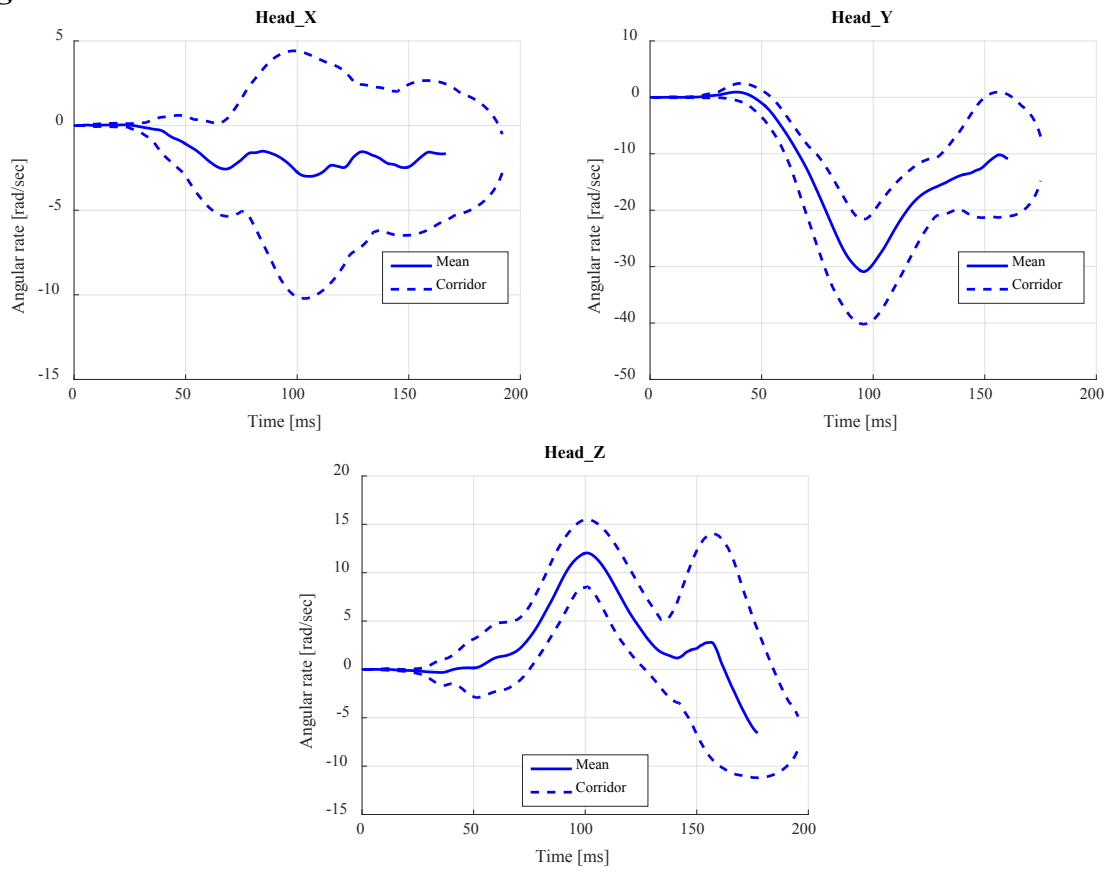


Figure 45. Head angular rate (unified)

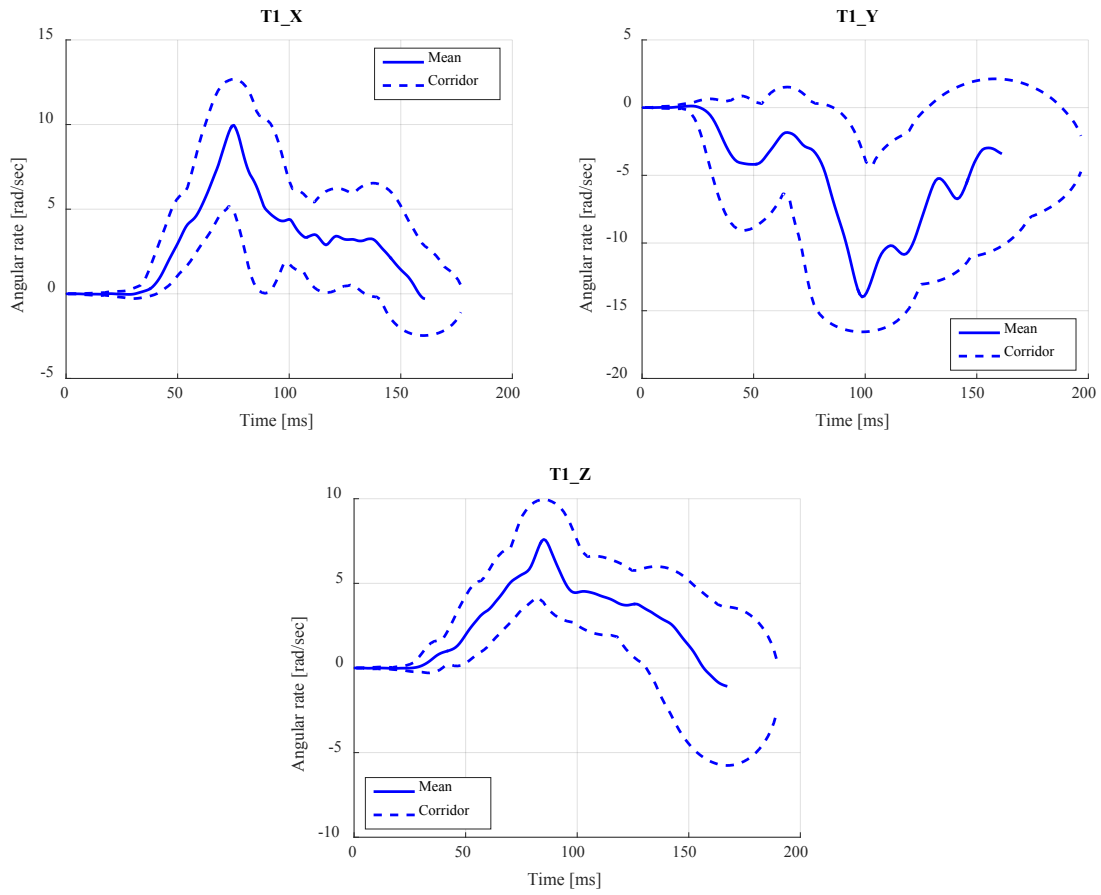


Figure 46. T1 angular rate (unified)

Acceleration

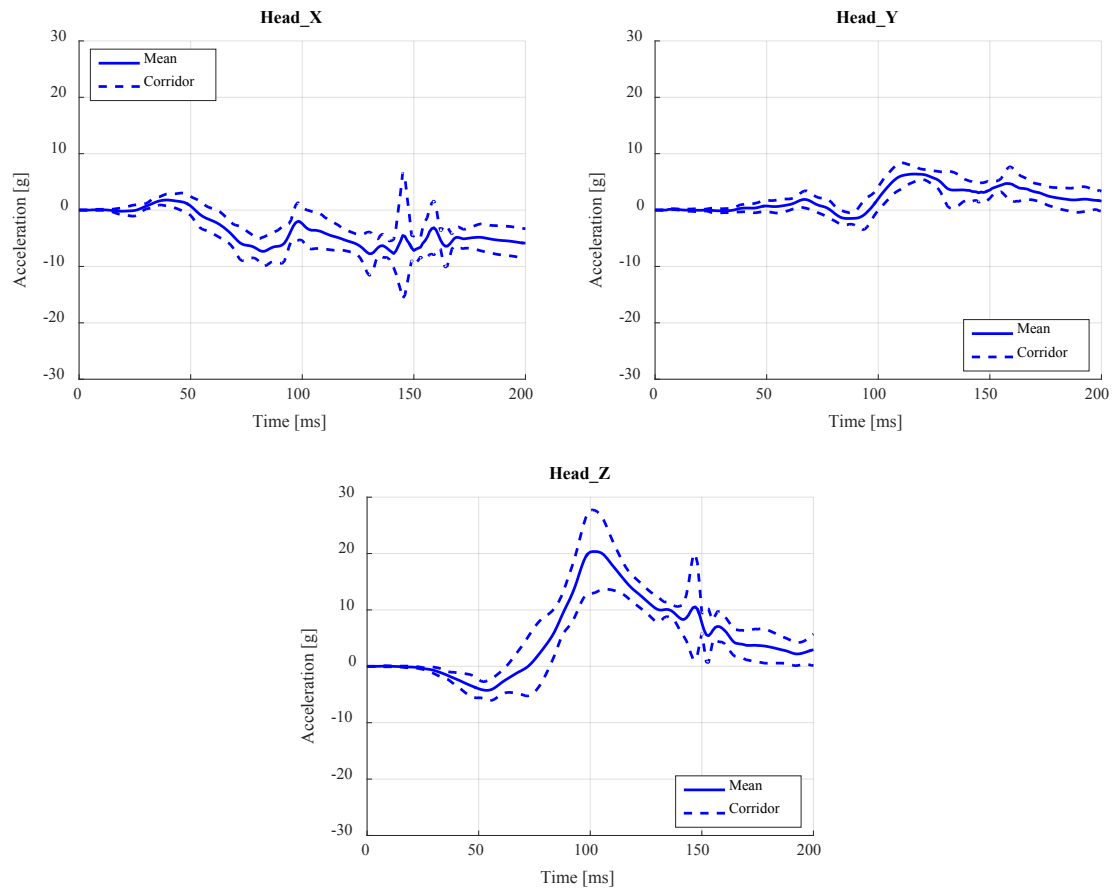


Figure 47. Head acceleration (unified)

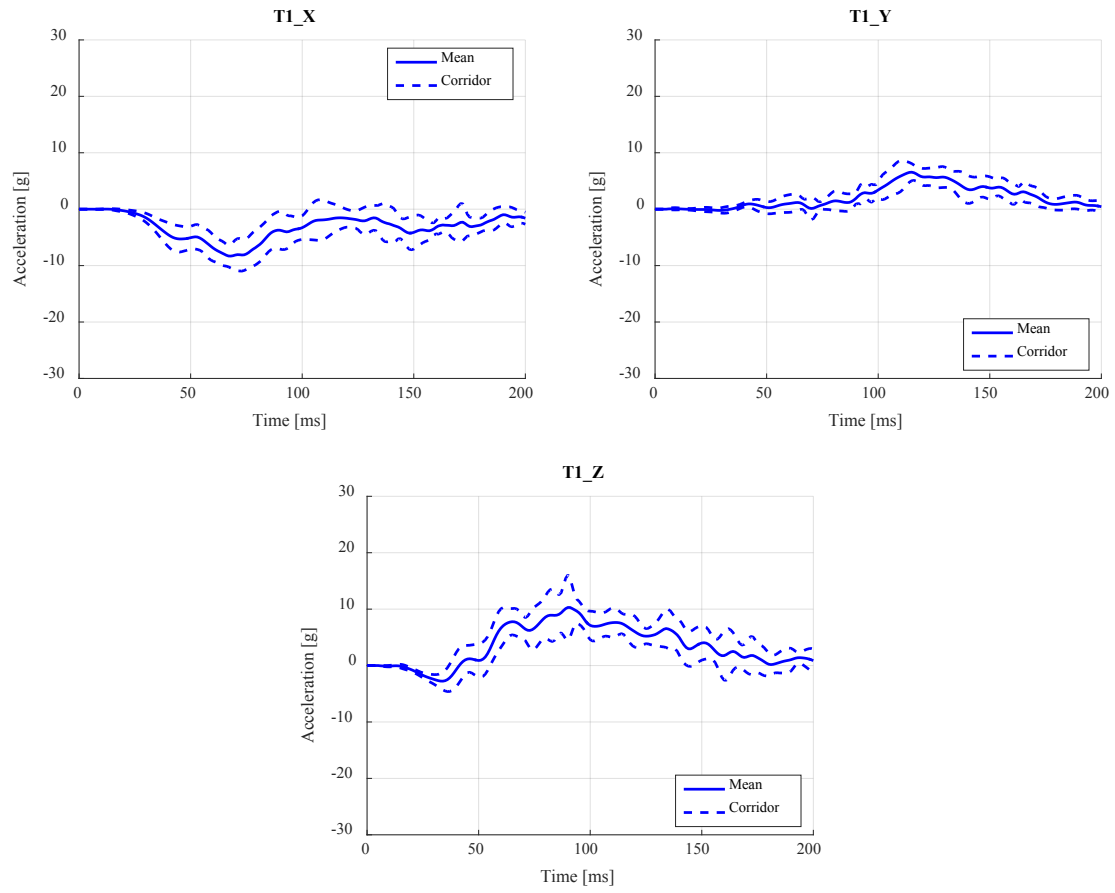


Figure 48. T1 acceleration (unified)

References

- Donlon, J. P., Jadooki, H., Toczyski, J., Lessley, D., & Forman, J. (2016). *Biofidelity corridors using arc-length parametrization to capture temporal variation among source time-histories and to facilitate analysis of cross-plots*. Presented at NHTSA's 44th International Workshop on Human Subjects for Biomechanical Research, on November 5, 2016, Washington, DC.
- Ash, J. H., Lessley, D. J., Forman, J. L., Zhang, Q., Shaw, C. G., & Crandall, J. R. (2012). *Whole-body kinematics: response corridors for restrained PMHS in frontal impacts*. Proceedings of IRCOBI Conference, September 12-14, 2012, Dublin, Ireland.
- Good, P. (2013). *Permutation tests: a practical guide to resampling methods for testing hypotheses*. Berlin: Springer Science & Business Media.
- Lessley, D. J., Crandall, J. R., Shaw, C. G., Kent, R. W., Funk, J. R. (2004). A normalization technique for developing corridors from individual subject responses (Paper 2004-01-0288). Warrendale, PA: Society of Automotive Engineers.
- Morgan, R. M., Marcus, J. H., & Eppinger, R. H. (1986, October). Side impact-the biofidelity of NHTSA's proposed ATD and efficacy of TTI. (SAE Technical Paper 861877). Warrendale, PA: Society of Automotive Engineers. DOI: 10.4271/861877
- Rhule, H. H., Donnelly, B., Moorhouse, K., & Kang, Y. S. (2013). A methodology for generating objective targets for quantitatively assessing the biofidelity of crash test dummies. 23rd Enhanced Safety of Vehicles Conference, May 27-30, 2013, Seoul, South Korea.
- Rhule, H. H., Maltese, M. R., Donnelly, B. R., Eppinger, R. H., Brunner, J. K. & Bolte, J. H. (2002). Development of a new biofidelity ranking system for anthropomorphic test devices. *Stapp car crash journal*, 46, 477-512.

Appendix A: Raw data

Thoracic Deflection (X)

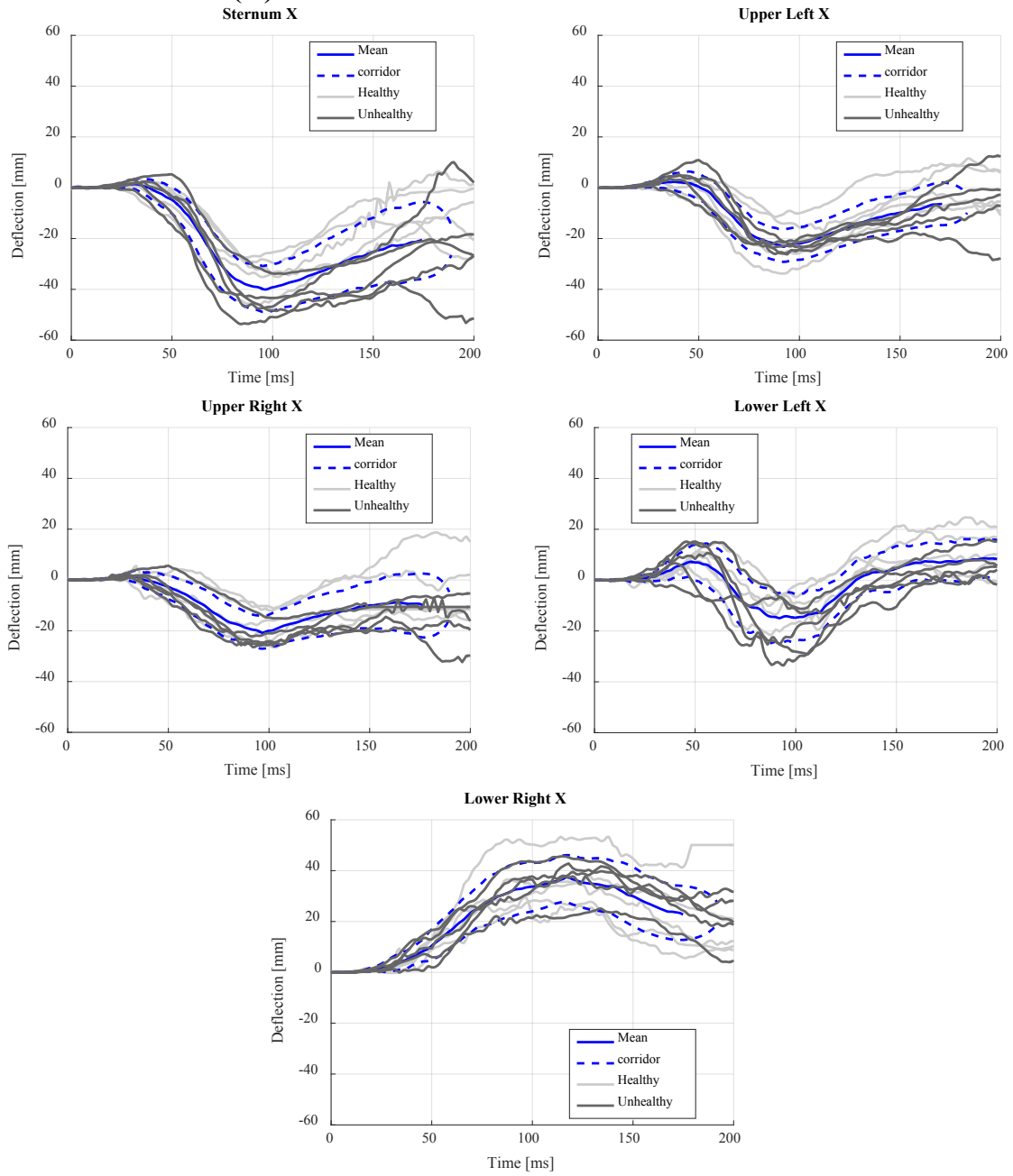


Figure 49. Thoracic Deflection (X)

Displacement of Anatomical Centers (X)

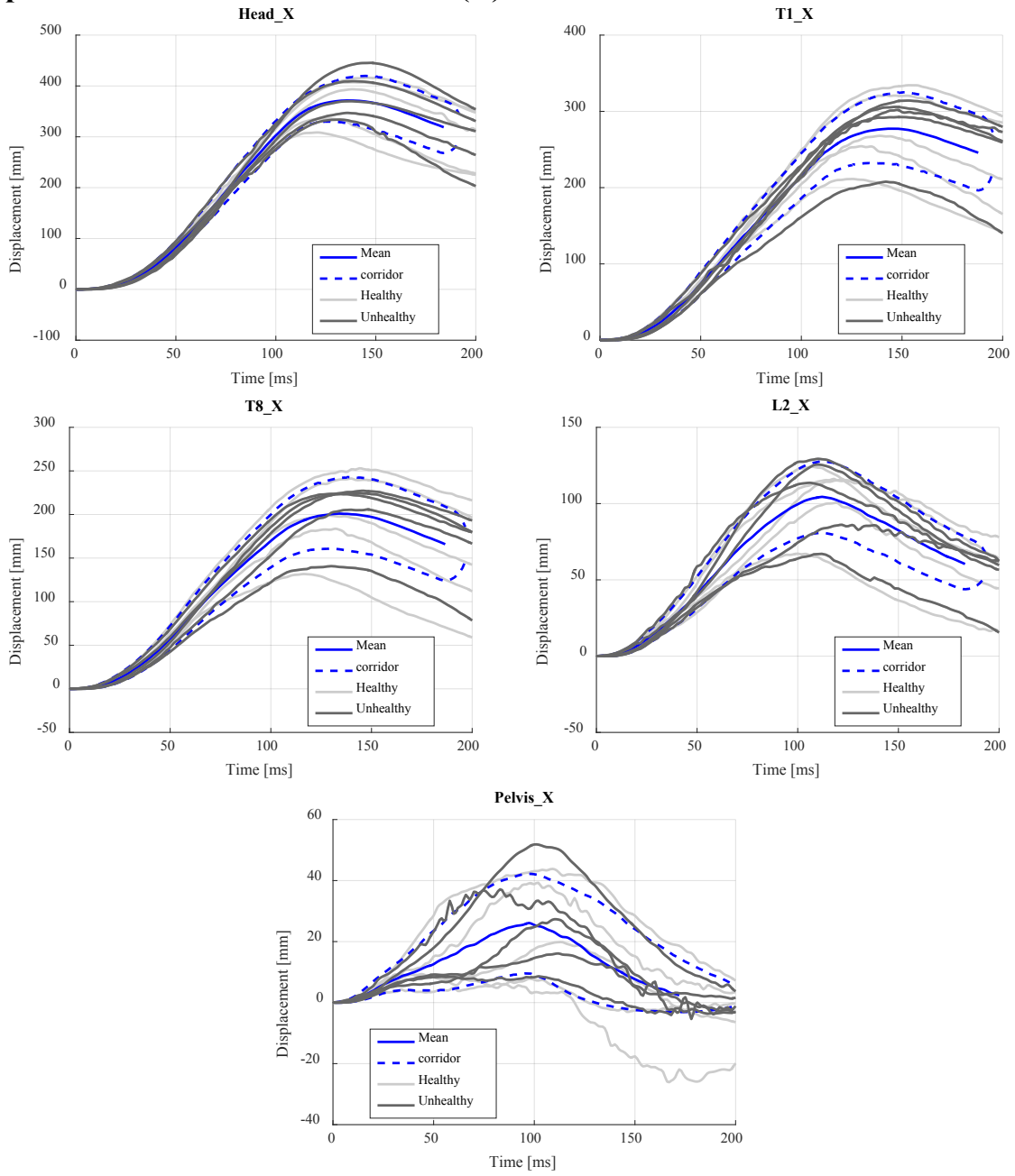


Figure 50. Displacement of anatomical centers (X)

Buck Load Cell

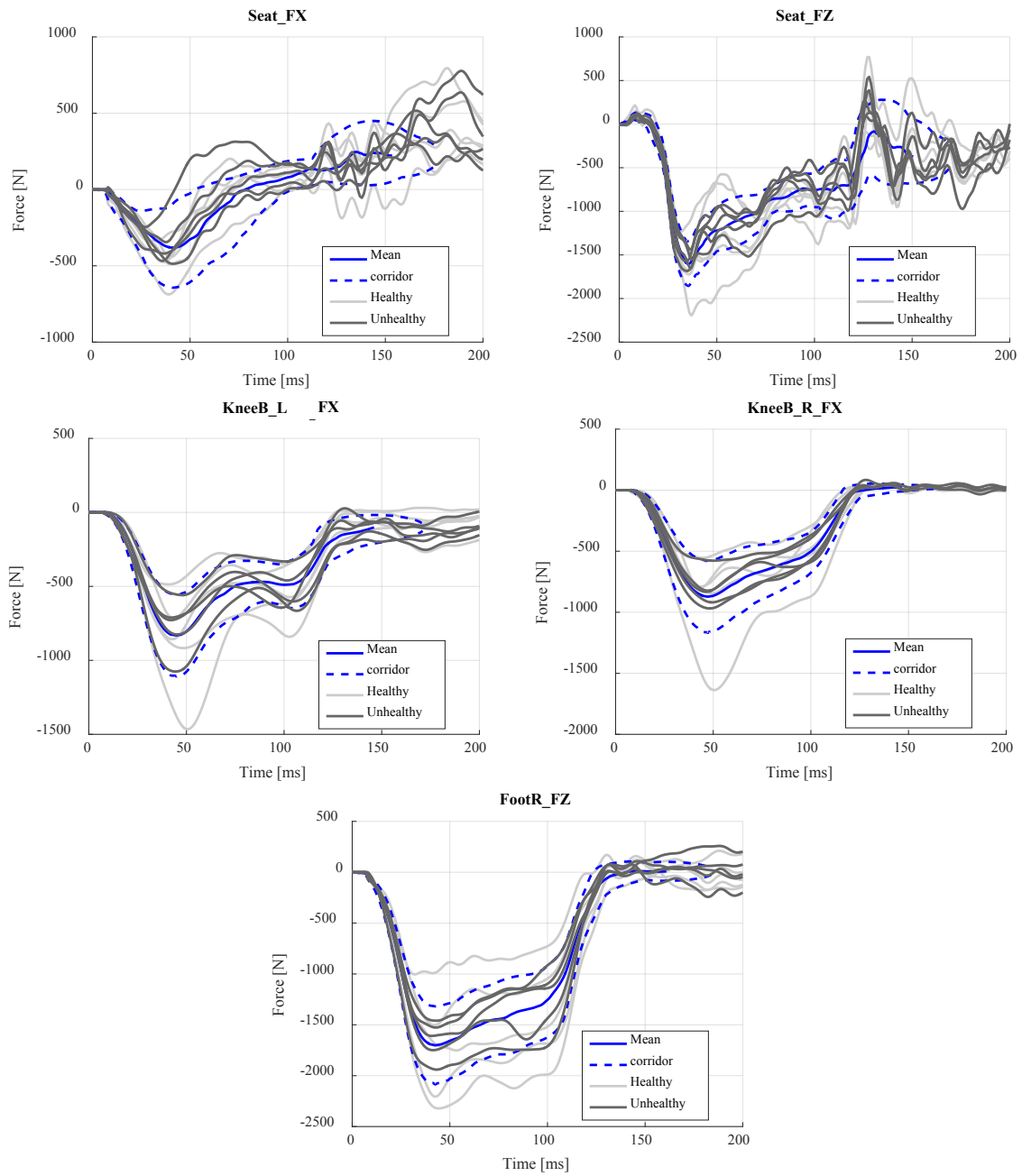


Figure 51. Buck load cell force

Belt Forces

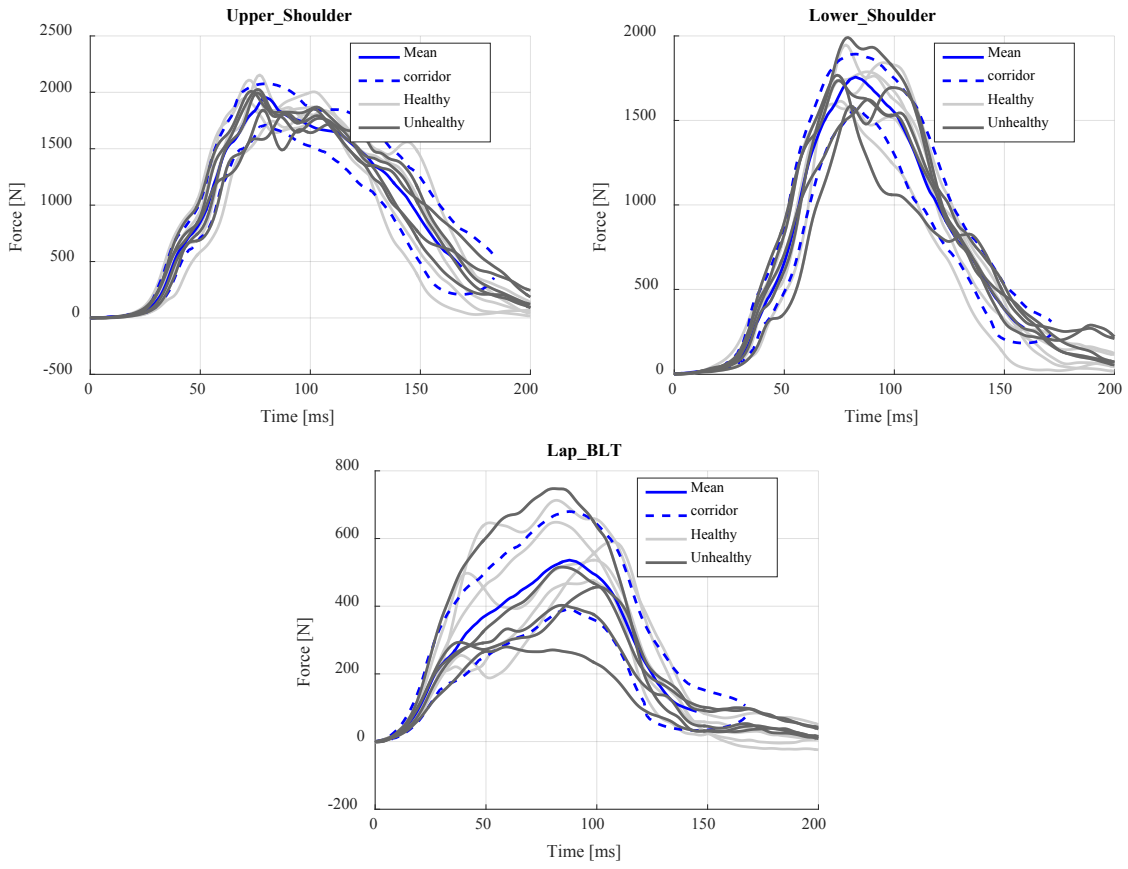


Figure 52. Belt force

DOT HS 812 743
July 2019



U.S. Department
of Transportation
**National Highway
Traffic Safety
Administration**

